NEVADA DOT

SAFE AND CONNECTED

Nevada Department of Transportation

Report No. 564-22-803

# Feasibility Study of Unmanned Aerial Vehicle Imagery for Mapping Roadside Milkweeds and Nectaring Plants for the Monarch Butterfly

August 2025

# Disclaimer

## TECHNICAL REPORT DOCUMENTATION PAGE

| | | |
|---|---|---|
| 1. Report No.<br>564-22-803 | 2. Government Accession No. | 3. Recipient's Catalog No. |
| 4. Title and Subtitle<br>Feasibility Study of Unmanned Aerial Vehicle Imagery for Mapping Roadside Milkweeds and Nectaring Plants for the Monarch Butterfly | | 5. Report Date<br>8/31/2025 |
| | | 6. Performing Organization Code<br>Click or tap here to enter text. |
| 7. Author(s)<br>Elizabeth Pringle, Tom Dilts, Hao Xu | | 8. Performing Organization Report No.<br>Click or tap here to enter text. |
| 9. Performing Organization Name and Address<br>Board of Regents<br>Nevada System of Higher Education (NSHE) on behalf of<br>University of Nevada Reno<br>1664 N Virginia St<br>Reno NV 89557 | | 10. Work Unit No. |
| | | 11. Contract or Grant No.<br>P564-22-803 |
| 12. Sponsoring Agency Name and Address<br>Nevada Department of Transportation<br>1263 South Stewart Street<br>Carson City, NV 89712 | | 13. Type of Report and Period Covered<br>Final Report<br>11/28/2022 to 8/31/2025 |
| | | 14. Sponsoring Agency Code |
| 15. Supplementary Notes<br>Click or tap here to enter text. | | |


16. Abstract

In this project, we sought to couple two imaging technologies, drones and vehicle-mounted cameras, with models using artificial intelligence to predict the location of milkweed plants in Northern Nevada. Milkweeds are weedy plants that frequently occur along roadsides, and they are the only food used by caterpillars of the monarch butterfly, whose populations have sharply declined in recent years. Conservation actions aimed at stabilizing populations of the monarch must thus identify the locations of milkweed plants. We conducted a pilot study using drones flown over three milkweed populations and determined that an artificial intelligence model aimed at identifying objects successfully identified individuals of two species of Western milkweed, although different methods were needed to identify flowering plants, whose nectar is needed by adult monarchs. This study also revealed that the abundance of narrowleaf milkweed predicts monarch presence. We conducted another study using images from the NDoT Roadviewer database and again successfully used object-based artificial intelligence to identify milkweed occurrence along Nevada roadways. It was, in general, easier to identify showy milkweed, which has a more distinctive architecture, than narrowleaf milkweed. Both studies revealed the importance of study timing relative to the life cycle of the milkweeds and monarchs.


| | | | |
|---|---|---|---|
| 17. Key Words<br>UAV, machine learning, convolutional neural networks, plant identification, milkweed, monarch butterfly | | 18. Distribution Statement<br>No restrictions. This document is available through the:<br>National Technical Information Services<br>Springfield, VA 22161<br>www.ntis.gov | |
| 19. Security Classif (of this report)<br>Unclassified | 20. Security Classif (of this page)<br>Unclassified | 21. No. of Pages<br>51 | 22. Price<br>n/a |

**Form DOT F 1700.7 (8-72)** Reproduction of completed page authorized NDOT Rev 08/2022

Project No. 564-22-803

# Feasibility Study of Unmanned Aerial Vehicle Imagery for Mapping Roadside Milkweeds and Nectaring Plants for the Monarch Butterfly

Final Report

Prepared for
Nevada Department of Transportation

by
Elizabeth G. Pringle
Thomas E. Dilts
Hao Xu
Gino Zamboni
Zhihui Chen
University of Nevada, Reno
Reno, NV

Victor King
Nevada Department of Transportation

August 2025

**ACKNOWLEDGMENT OF SPONSORSHIP**

This work was sponsored by one or more of the following as noted:

- ☒ American Association of State Highway and Transportation Officials, in cooperation with the Federal Highway Administration, and was conducted in the National Cooperative Highway Research Program,
- ☐ Federal Transit Administration and was conducted in the Transit Cooperative Research Program,
- ☐ Federal Aviation Administration and was conducted in the Airport Cooperative Research Program,
- ☐ The National Highway Safety Administration and was conducted in the Behavioral Traffic Safety Cooperative Research Program,

which is administered by the Transportation Research Board of the National Academies of Sciences, Engineering, and Medicine.

**TABLE OF CONTENTS**

**List of Tables and Figures**

**Author Acknowledgments**

The research reported herin was performed under agreement 564-22-803 by the Board of Regents, Nevada System of Higher Education, on behalf of the University of Nevada, Reno (UNR).

Dr. Elizabeth Pringle, Associate Professor of Biology at UNR was the Project Director and Co-Principal Investigator. The other authors of this report are: Thomas Dilts, Research Scientist in the Department of Natural Resources and Environmental Science at UNR and Co-Principal Investigator; Dr. Hao Xu, Professor of Civil and Environmental Engineering at UNR and Co-Principal Investigator; Gino Zamboni, Research Assistant and master's student at UNR; and Zhihui Chen, Research Assistant and PhD candidate at UNR, and Victor King of the Location Drone Team at the Nevada Department of Transportation. During the course of this work, Gino Zamboni received his master's in Ecology, Evolution and Conservation Biology from UNR, and Dr. Zhihui Chen received his PhD in Civil and Environmental Engineering from UNR and now works for the California Department of Transportation.

Nevada Department of Transportation (NDOT) Research funded the project. Christopher Young and Nova Simpson served as project champions. Mitch Ison, Lucy Koury, and Melissa Demattei provided administrative support from NDOT. Victor King led the UAV photography, and Erika Johnson provided support. Members of the Location Drone Team piloted the UAV aircraft and collected data in the field and helped to process data in the office. Casey Smith and Kyle Bacon provided images from Roadviewer. Nova Simpson and Sabra Gilbert-Young provided significant feedback throughout the project. Jessica Abbott and Carl Lunderstadt provided access to the Walker Basin Conservancy and the Stillwater National Wildlife Refuge Complex, respectively. Washoe Lake State Park gave permission for UAV flights.

**Abstract**

This project sought to couple two imaging technologies, drones and vehicle-mounted cameras, with models using artificial intelligence to predict the location of milkweed plants in Northern Nevada. Milkweeds are weedy plants that frequently occur along roadsides, and the milkweeds are the only food used by caterpillars of the monarch butterfly, whose populations have sharply declined in recent years. Conservation actions aimed at stabilizing populations of the monarch must thus identify the locations of milkweed plants. This report describes a pilot study using drones flown over three milkweed populations and determined that an artificial intelligence model aimed at identifying objects successfully identified individuals of two species of Western milkweed, although different methods were needed to identify flowering plants, whose nectar is needed by adult monarchs. This study also revealed that the abundance of narrowleaf milkweed predicts monarch presence. This report also describes another study using images from the Nevada Department of Transportation (NDOT) Roadviewer database and again successfully used object-based artificial intelligence to identify milkweed occurrence along Nevada roadways. It was, in general, easier to identify showy milkweed, which has a more distinctive architecture, than narrowleaf milkweed. Both studies revealed the importance of study timing relative to the life cycle of the milkweeds and monarchs.

**Summary**

The monarch butterfly has been gaining national attention as population declines from 75-85% have been documented across its range. It is a proposed threatened species under the Endangered Species Act (ESA). Once protected under the ESA, all state or federal activities that intersect with monarch habitat must be reviewed for impacts and either Section 10 (state) or Section 7 (federal) consultations will be required. These consultations are time-consuming and costly and could be required for all actions from small maintenance projects to large road projects. Due to the pending listing, a nationwide Candidate Conservation Agreement with Assurances (CCAA) was developed in collaboration with USFWS. This effort allows landowners and land managers (including property owners, easement holders, and lease holders) to voluntarily commit to conservation actions with the intention of addressing the needs of the monarch before a listing is issued (www.fws.gov). In return, USFWS provides participants with an Enhancement of Survival permit containing assurances that they will not be required to implement additional conservation measures beyond those in the agreement when the species becomes eligible for full protection under the ESA (www.fws.gov).

To participate in the monarch CCAA, the landowners and land managers must document suitable habitat and decide what areas will be covered under the agreement (i.e., enrolled acres) and implement best management practices on a portion of that habitat that will benefit the monarch butterfly (i.e., adopted acres). The applicant must develop an implementation plan for the adopted acres and perform yearly surveys on a subset of the adopted acres, which require counting both milkweeds and flowering plants during the growing season. Traditional survey methods require a biologist to walk a random transect and document plant diversity and nectar species cover, but this is labor-intensive and must be completed during the appropriate growing seasons. Because the growing seasons in Nevada are short and staff are limited, here the team investigated new photographic and artificial-intelligence-assisted technologies that would help staff identify milkweed populations, assess their potential for use by monarch butterflies, and complete the required surveys in a relatively short time frame.

In this research project, the team investigated two new technologies for mapping milkweed populations. The first is the use of unmanned aerial vehicles (drones or UAVs) for mapping milkweed and understanding monarch habitat use at three intensively studied sites. The team compared traditional field methods with those made possible by UAV flights and accompanying analysis assisted by artificial intelligence (including both machine-learning and deep-learning analyses). In addition, the team assessed the ability of the deep-learning artificial intelligence algorithm (YOLO) to identify roadside milkweed using photographs from the Nevada Department of Transportation's Roadviewer database for state-managed highways. Although the Roadviewer database was originally developed for asset management, the team here tested its use for mapping roadside milkweed populations. Milkweed locations derived from Roadviewer and population sizes determined by UAV flights and accompanying analyses can be incorporated into the Nevada Department of Transportation's (NDOT's) adopted acres to fulfill their CCAA requirements.

Both studies produced results with a high degree of accuracy. The UAV study demonstrated that UAVs are a useful tool for censusing milkweeds and can be used to map floral diversity and cover in addition to narrowleaf and showy milkweed. This allows for accurate counts of milkweeds with a very high degree of accuracy (~90%). The results additionally showed relationships between milkweeds and monarch habitat use, with narrowleaf milkweed being the better predictor of monarch occurrence of the two milkweed species. Interestingly, it also appeared that UAVs provided less biased estimates of milkweed cover in plots compared to observer surveys on the ground because the UAV imagery is downward looking.

Data from the Roadviewer database, when coupled with artificial intelligence and image augmentation techniques, was able to predict milkweed presence with 86 to 93% accuracy. Adjustments to the images, including augmentation of image brightness, and to the analyses, including filtering images that had more model-predicted occurrences of the plant, increased the accuracy of milkweed identification. Roadviewer imagery could thus be used to guide mowing and herbiciding treatments to avoid milkweed as part of the CCAA, especially later in the summer when monarch eggs and caterpillars might be on the milkweed. Although it was beyond the scope of this study, the results here suggest that repeat Roadviewer imagery could be used to determine whether milkweed is increasing or decreasing along NDOT-managed roadsides and whether NDOT management is having an impact on milkweed populations.

In summary, these two imaging approaches, assisted by emerging technologies from artificial intelligence, can provide cost-effective approaches for mapping milkweed area, prioritizing areas to avoid herbicide and mowing in the late summer, and developing long-term monitoring to determine whether NDOT actions are affecting milkweed populations. Roadviewer imagery is appropriate for broad-scale mapping and monitoring whereas UAV imagery is appropriate for smaller more targeted sites in which milkweed counts are needed. By leveraging advanced technologies, NDOT has emerged as a national leader in the science and management of roadside milkweeds.

## CHAPTER 1: UAV Study Background

The proliferation of UAV (unmanned aerial vehicle), otherwise known as “drone,” technology has prompted novel methods of data collection and analysis for a wide variety of fields. More specifically, UAVs have seen increased usage in professions that make use of remote sensing for data collection, where UAVs offer some advantages relative to traditional aircraft survey methods and satellites (Behera et al. 2023). Crewed aircraft allow for a large area to be covered in a single flight and can carry sophisticated remote sensing technology, such as lidar. However, aircraft suffer from prohibitive costs, crew safety concerns, and limited deployment flexibility. Satellite data is lower cost and can be used to monitor areas over long time periods, but satellite imagery is limited by its low spatial and temporal resolution (Gautam et al. 2025). Challenges with these remote-sensing methods make it difficult to collect information about finer-scale spatial variables, such as the cover of individual species, flowering species area, and species diversity. UAVs avoid many of these operating issues: they are significantly cheaper to fly, relatively easy to use and deploy, and flexible in where and when they can be flown, allowing data collection that can be targeted to the phenology of focal species (Weisberg et al. 2021). The primary advantage of UAVs is their ability to collect high-resolution spatial data, including the ability to identify specific forms of vegetation that may be lost with coarser-resolution platforms (Hosseiny et al. 2020).

UAVs have been used for collecting a wide range of ecological and natural resource data and have been widely used for mapping rare and invasive species of concern. One such application is collecting data on the distribution of invasive species like Siam weed (*Chromolaena odorata*) in Australia (Gautam et al. 2025). UAVs are also utilized in agricultural settings—for example, they have been used to identify the toxic flowering plant *Colchicum autumnale* in pastures and meadows to protect livestock (Lukas et al. 2020). High-resolution data from UAVs can also permit identification of rare species that would traditionally be difficult to locate in the field, such as the dwarf bear-poppy (*Arctomecon humilis)*, an endangered flowering plant species in the Utah desert (Rominger and Meyer 2019). With data collection from UAV’s becoming more common, new methods for the analysis of these data have also appeared. In particular, convolutional neural networks (CNNs) have become very popular for modeling UAV data using machine learning. Optical camera imagery in red, green, and blue (RGB) from UAVs are adequate for many vegetative classification problems and are more cost effective than other options such as hyperspectral cameras (Gautam et al. 2025). Machine learning provides advantages over traditional methods of identifying plant species by being significantly less time-consuming, potentially allowing plant identification over much larger areas. They also reduce costs, minimize labor, and reduce the potential for human error, which can enhance reproducibility (Hosseiny et al. 2020).

Beyond identifying individual plant species, UAV data is increasingly being used to assess broader ecological patterns, such as plant community structure and even species interactions. For example, UAVs have been used to map vegetative communities in the raised bogs of Ireland, to classify vegetation in southwestern US forests, and to estimate biodiversity in the Zao mountains of Japan (Sankey et al. 2017, Bhatnagar et al. 2020, Conciatori et al. 2024). It remains less clear whether more traditional identification via UAVs of individual plant species could sometimes be used to predict the diversity of plant communities. It is likewise uncommon to use UAV identification of individual plant species to predict species interactions. For example, using the abundance of a specific plant species to predict the distribution of an animal species that utilize it for food. Generally, UAVs have not received much scrutiny as a tool for measuring plant-insect interactions, despite the obvious dependence of many insect species on plants.

Pollinating insects play a critical role in providing ecosystem services that benefit humans and maintain biodiversity. However, relatively few studies have attempted to link pollinating insects to vegetation communities using UAV-derived data. Linking UAV imagery to the abundance or diversity of pollinating insects is likely more challenging because many pollinators can utilize a wide variety of flowering species for food. Likewise, an individual plant species may host the larval forms of many insect species. Nevertheless, UAV data have been used to demonstrate that heterogeneity of vegetative height in grasslands can effectively predict flower and bee diversity (Torresani et al. 2024). A key open question in this field is how best to scale up from observations of individuals to broader site-level patterns using UAV-derived data. Addressing this question will require clear strategies for connecting fine-scale interactions—such as those between individual plants and pollinators—to larger landscape patterns. Importantly, some pollinators rely on specific host plants, and the presence of these hosts may have a disproportionate effect on the local abundance of those specialist insect species. UAV-based approaches may prove especially useful in cases where specialist insects are closely tied to identifiable plant hosts.

One such specialist plant-insect system is that of milkweed plants and monarch butterflies. The relationship between milkweed plants (*Asclepias* spp.) and monarch butterflies (*Danaus plexippus*) is a clear example of a plant-insect interaction with conservation relevance. The caterpillar larvae of monarch butterflies are specialists of milkweed plants in the genus *Asclepias*. Following metamorphosis, adult monarchs nectar on a wide variety of flowering plant species. Monarch butterfly populations have faced decline in recent decades and are now under consideration for listing as an threatened species (Flockhart et al. 2015, Crone et al. 2019). Milkweed habitat is also being reduced by herbicide use in agricultural fields, management of roadsides, and development of former habitat areas (Pleasants and Oberhauser 2013, Lalonde et al. 2022). Mapping high-quality milkweed sites and understanding patterns of monarch breeding habitat use is critical for ensuring the long-term viability of this species.

In this study, using imagery from a UAV, the project team attempted to map the distribution of two milkweed species along with floral cover and floral diversity, as well as relate these vegetation variables to field-derived monarch counts. In particular, the project addressed whether UAV imagery allows for mapping of milkweeds and floral resources, and whether these patterns are predictive of monarch habitat use at relatively fine spatial scales. The project team also conducted traditional field surveys to validate our UAV data and machine learning models and compare the efficacy of a combined field-survey and imagery approach against field data alone. The predictions of the study were as follows. First, that these new methods would accurately estimate milkweed cover of two common species (*Asclepias fascicularis* and *Asclepias speciosa*) as well as floral cover and floral species richness. Second, that the vegetative variables at the levels of individual plant and floral community would successfully predict monarch abundance, but that milkweed cover would be a stronger predictor of monarchs, a specialized herbivore, than variables describing the broader floral community.

## CHAPTER 2: UAV Study Research Approach

Three sites were surveyed in summer 2023. The sites were chosen to have relatively large populations of milkweed plants and monarch butterflies. The sites were distributed among three major basins in western Nevada: Stillwater Wildlife Refuge (Lahontan Valley, hereafter "Stillwater;" 39.531301, -118.519812), Washoe Lake State Park (Located between Reno and Carson City, hereafter "Washoe Lake;" 39.239975, -119.767970), and one site located on lands owned by the Walker Basin Conservancy in Smith Valley, Nevada (Hereafter "Smith Valley;" 38.795074, -119.372062) (Figure 1). The focal milkweed species were narrowleaf milkweed (*A. fascicularis*) and showy milkweed (*A. speciosa*). The density of the two focal milkweed species and existing features, such as canals, lakes, and roads, were used as boundaries to define each site. The sites differed in size, Stillwater was 12.69 ha; Washoe Lake was 3.18 ha; and Smith Valley was 1.96 ha. Both species of milkweed were present at Stillwater and Smith Valley, but *A. speciosa* was not present at Washoe Lake. The Stillwater site spanned an abandoned agricultural field and active irrigation ditch; Washoe Lake comprised a weedy field ending in a sandy embankment at the edge of Washoe Lake; Smith Valley encompassed the length of an inactive irrigation ditch system.

Maps were prepared in Quantum GIS (QGIS Development Team 2023) comprising grid cells (plots) that were approximately 10x10 meters covering each site and used QField (OpenGIS.ch 2023) on Android and iOS phones to select plots from evenly spaced grids at each site. The initial aim was to search 25 randomly selected plots at each site but ended up surveying $n$ = 27 plots at Stillwater, $n$ = 42 plots at Washoe Lake, and $n$ = 29 plots at Smith Valley. The total area of the surveyed plots at each site was 1,603.5 $m^2$ for Stillwater, 4,200.0 $m^2$ for Washoe Lake, and 1,759.5 $m^2$ at Smith Valley.

Between June and October 2023, the project team performed seven field surveys and three UAV-imaging flights at each site with field surveys co-occurring with UAV flights and additional field surveys spaced roughly two weeks before and after flights (Table 1). For the field surveys, vegetation and monarch data were collected in each of the selected ~10x10 m plots. Within each plot, the following data were recorded: (1) the percent cover of flowering plants; (2) the number of flowering species; (3) the percent cover of each species of milkweed; and (4) the number of monarch individuals as eggs, larvae, and adults. The percent cover of flowering plants and milkweeds were visually estimated after marking the boundaries of each plot. The number of flowering species was determined by exhaustively searching the plot for unique flowering plant species. Finally, all milkweed stems were searched for monarch eggs and larvae and any adults flying through the plot were noted in the standardized search time of 3.5 minutes. Data was entered into the Qfield phone app to record GIS locations of all variables and uploaded into QGIS upon return to the office.

Prior to each UAV flight, the project team distributed ground control points evenly throughout the survey area. There were 10 ground control points at Washoe Lake and 15 at both Stillwater and Smith Valley. The UAV flew concurrently while field crews were collecting data on site. There were two flight plans performed at each sampling date, and the flight line directions were set at 45° offset to one another. The time for an individual flight varied by site according to its size: 40 min at Stillwater; 20 min at Washoe Lake, and 15 min at Smith Valley. Flight dates were selected to be roughly one month apart to capture phenological differences of the plant species and were conducted under clear sky conditions to ensure uniform levels of illumination. All flights were conducted between 10 am and 2 pm in order to minimize shadows and avoid late afternoon wind. The Washoe Lake and Smith Valley sites were flown on the same day during each field campaign and Stillwater was flown one day prior.

The UAV flew 23 m above ground level at Washoe Lake and Smith Valley, and at 26 m at Stillwater, to account for some large trees. A DJI Phantom 4 Pro UAV model was used for Washoe and Smith while both the DJI M200 and DJI Phantom 4 Pro models were used for

Stillwater. The addition of the second model of UAV (the DJI M200) for Stillwater was to accommodate for the higher elevation flights needed at this site. To ensure accurate mosaicking the side and forward overlap of the images was 65% at all three sites. For each site, the UAV collected three spectral bands in the red, green, and blue wavelengths (RGB). Pix4d Mapper software was used to develop the orthomosaic maps for Washoe Lake and Smith Valley (Pix4D SA 2023). Virtual Surveyor – Terrain Creator was used to develop the map for Stillwater (Virtual Surveyor NV 2023). Stillwater required a different program because most of the site was comprised of largely uniform vegetation, which caused challenges with image alignment and distortion in Pix4D**.** Virtual Surveyor addressed these issues by providing tools for manual terrain correction and refinement.

Data from the field surveys were combined across all dates. Due to the low frequency of monarch occurrences, the number of larvae, eggs, and adults recorded for each plot were summed across all time points to create a value for "monarch abundance." The mean values of percent floral cover, number of floral species, percent cover of *A. fascicularis*, and percent cover of *A. speciosa* for each plot were also calculated over all time points. To estimate milkweed abundance using the UAV data, the orthomosaic maps for each site were used to both: (i) manually identify milkweed plants and (ii) predict their occurrence using machine learning. For manual identification, one project team member (GZ) scanned the three orthomosaic images by eye. Polygons were manually drawn around the entire area of each identified plant as bounding boxes. To determine if similar polygons could be identified using machine learning, a convolutional neural network called YOLO (Jocher and Ultralytics 2025), which uses convolutional filters to analyze images in layers and extract important patterns like edges, textures, and complex shapes, was applied to the data.

For YOLO analysis, the sites were segmented into 1,569 5x5 m grids. These grids fell into two categories, images containing visible milkweed and images that did not. The grids were split into 70% training data and 30% test (*i.e.*, validation) data. Due to a small sample size the data were split into only training and testing sets rather than into training, testing, and validation sets. The model utilized the manually identified data from the test grids after resizing them to a 640x640 pixel resolution and normalizing the pixels in each RGB channel to be either 0 or 1. The RGB channels were normalized by subtracting the channel-wise mean and dividing by the standard deviation. The normalization step provides a consistent distribution of values, which ensures that each pixel value contributes to the model's performance without causing instability or bias during training. The manually identified and YOLO outputs were then compared to generate polygons classified as true positive, false positive, and false negative across the orthomosaic images for each site and for each milkweed species. True positives were YOLO polygons that identified the same milkweed as the manually identified output, false positives were YOLO polygons that identified milkweed that did not exist in the manually identified output, and false negatives were manually identified milkweeds that the YOLO model had missed (Figure 1). The YOLO model was analyzed by taking the YOLO true positive, true negative, false positive, and false negative area values and using them to calculate precision, recall, F1 score and total accuracy for the model across both species at each site.

As it was impossible to visually identify flowers in the orthomosaic images for many of the species due to the resolution of the imagery (7.35–8.49 mm/pixel), floral richness and cover from the orthomosaic images were estimated using image segmentation and random forest. Object-based image segmentation was conducted using the orthomosaic images from 25 July, which had the highest flowering plants cover in the field surveys (Blaschke 2010), to describe the spectral and spatial attributes of distinct vegetation clusters and then use those attributes to perform a random forest regression to predict floral richness and floral cover (Breiman 2001). The first step of segmentation was calculated using the Segment Mean Shift tool in ArcGIS Pro version 3.1 (Esri 2024). Mean shift segmentation was performed individually using the July orthomosaic images as the basis for the segmentation using default parameters (spectral detail

= 15.5, spatial detail = 15, minimum shift size = 20). The segmented image for each study area was converted to polygons and zonal statistics were performed in ArcGIS Pro 3.1 to calculate the mean and standard deviation of the red, green, and blue bands for each flight date for each image segment (polygon). In addition to the spectral variables, the Compute Segment Attributes tool in ArcGIS Pro 3.1 was run to calculate the average segment size and compactness for each segment. A second zonal statistics analysis was performed to summarize the spectral and spatial attributes for the 10x10 meter sampling blocks across all three study areas.

To create models of floral richness and diversity, the data were pooled across study areas and created random forest regression models individually for floral species richness and floral species cover using the 96 surveyed plots as training and testing data. Random forest has been shown to suffer when the distribution of training data is highly skewed (Valavi et al. 2021) as was the case for our plots (low levels of floral cover and floral richness were far more common than plots with high values). To correct for class imbalance in these models we divided the dataset into ten equal interval bins for each response variable (floral species richness, floral species diversity) and we duplicated (upsampled) data using random sampling with replacement, to produce an equal number of samples for each bin. Using the Forest-based Classification and Regression tool in ArcGIS Pro 3.1 we created predictive models for floral species richness and floral species diversity using 90% of the plots for training and 10% for validation. In addition to training and testing the model, we also created predictive maps of floral species richness and floral species diversity for each 10x10 meter box across each of the three study areas. Due to the duplication, we acknowledge that cross-validation using the random forest is optimistically biased while our small number of testing plots (n=88) makes our model testing results subject to outliers.

Statistical analyses were conducted in R version 4.3.3 (R Core Team 2024). We examined correlations among our estimates of plant and floral cover using correlations from R's base stats package. In all cases, we assessed the correlation between two floral/plant predictors. Because there were 28 such pairs, significance was assessed using a Bonferonni correction ($\alpha$ = 0.05/28 = 0.002) to reduce the likelihood of type 1 errors. To predict monarch abundance using our vegetative variables, we used penalized regression in the glmnet package (Friedman et al. 2010). To account for unmeasured effects of site on monarch abundance, we first fit a mixed-effects intercept model with site as a random intercept using glmer from the lme4 package and extracted the residuals (Bates et al. 2015). We used these residuals as the response variable in an elastic net regression model ($\alpha$ = 0.5). To account for the high correlations among our three methods of estimating milkweed cover, we extracted the first principal component of the three estimation methods (field, manual, YOLO) for *A. fascicularis* and *A. speciosa*, respectively. We then used these two principal components, along with floral cover and richness, as our predictors. We assessed model performance with cross-validation to find the optimal regularization level. The final model coefficients were drawn from predictors that were retrained at the lambda that minimized mean cross validated error. After finding that *A. fascicularis* cover was the best predictor of monarch counts, we used generalized linear models with a negative binomial distribution to visualize the effect of the three different estimation methods (Brooks et al. 2017). In these models, total monarch count for each plot was the response variable, and the floral/plant variable was the predictor, with site treated as an additional fixed effect. Several landscape metrics were generated for both species and GLMMs set up identically to those mentioned above were used to investigate potential relationships with monarch count.

## CHAPTER 3: UAV Study Findings and Applications

The YOLO model applied to the UAV-generated orthomosiac images accurately estimated the cover of both narrowleaf and showy milkweeds (Table 2). There were strong associations among all three methods of determining milkweed cover—field surveys, manually identified from the orthomosaic images, and YOLO-identified from the orthomosaic images—for both milkweed species (Table 2). These six correlations maintained statistical significance after Bonferroni corrections. A comparison between the field survey estimations and those from the UAV, whether manually identified or using the YOLO model, revealed a consistent overestimation of milkweed percent cover in field surveys. On average, field estimates of narrowleaf cover were 14.5 times greater than values manually identified from the orthomosaic images and 13.7 times greater than YOLO estimates. Similarly, field estimates of showy milkweed cover were 14.9 times greater than manual interpretations and 18.6 times greater than YOLO-derived estimates. No significant associations were found between the percent cover of narrowleaf and showy milkweed, regardless of estimation method. The YOLO model generally did well with both accuracy (0.997 – 0.999) and precision (0.566 – 0.825) at Stillwater and Washoe Lake (Figure 2; Table 3): F1 scores, which represent the harmonic mean of accuracy and precision, at these sites were above 0.7 (Table 3). In contrast, the model had a hard time predicting the occurrence of either milkweed species at Smith Valley, where most of the vegetation was densely crowded within an agricultural ditch with tall overlapping vegetation on both sides of the ditch. This can be seen through the low F1 scores for narrowleaf (F1=0.021) and Showy (F1=0.113) at Smith Valley (Figure 2; Table 3).

Although the floral richness and cover variables could not be mapped using the orthomosaic images directly (i.e. individual flowers from most species were smaller than the 7 or 8 mm pixels size), the predictions from the random forest model using object-based image analysis showed positive associations between these estimates and field estimates of both floral cover and species richness (Figure 3). The weak R-squared value ($R^2 = 0.05$) for the floral cover correlation was principally the result of a single outlier from Smith Valley (Figure 3B). The correlations among vegetation variables also provided insight into the association between milkweed cover and floral variables at our sites. Of the showy variables only field showy had an association with a floral variable, as it displayed a weak negative association with floral cover. Manual narrowleaf had a weak positive association with both floral cover and floral richness, which were the only associations between narrowleaf and floral variables (Table 2). Field floral cover also showed a strong positive relationship with field floral richness (Table 2).

Monarch abundance was positively associated with narrowleaf milkweed cover, regardless of the estimation method ($\beta = 0.32$) (Figure 4; Figure 5). The narrowleaf variables displayed the strongest relationship with monarch abundance and these associations were individually visualized (Figure 5). In contrast, no relationships were detected between showy milkweed cover and monarch abundance. Floral richness was also positively associated with monarch abundance ($\beta = 0.066$) but floral cover was not. None of the estimations of showy milkweed cover were related to monarch abundance. Several of our narrowleaf landscape metrics were significantly associated with monarchs including mean shape index ($\beta = 1.088$, z-value = 2.623, p-value = 0.009) (Table 4), which indicates that the average patch complexity is positively associated with monarch count. Mean Euclidean nearest neighbor was also important ($\beta = -0.26$, z-value = -2.925, p-value = 0.004), this indicates that plots in which patches were further apart tended to have fewer monarchs. Of these narrowleaf landscape metrics, nearest neighbor within 5 meters mean was the most significantly associated with monarch count ($\beta = -0.384$, z-value = -3.845, p-value = 0.0001). This negative relationship implies that denser narrowleaf patches increase monarch presence. There was also significant variation in the abundance of monarchs among sites, as well as in the life stages in which the monarchs were most commonly observed. Washoe Lake had the most monarchs, followed by Smith Valley, with the fewest monarchs observed at Stillwater. At Washoe Lake and Smith Valley, monarchs were observed in all three life stages, and more larvae were observed than adults or eggs. Curiously, at Stillwater, we observed only adult monarchs; no larvae or eggs were found at this site despite the prevalence of both narrowleaf and showy milkweed. This difference resulted in a significant effect of site in models predicting monarch abundance with narrowleaf milkweed cover (field: $\chi^2 = 14.32$, df = 1, $P < 0.0002$; manual: $\chi^2 = 15.16$, df = 1, $P < 0.0001$; YOLO: $\chi^2 = 17.16$, df = 1, $P < 0.0001$).

## CHAPTER 4: UAV Study Conclusions and Suggested Research

In this study, we examined a new method of using UAV image data and machine learning to map milkweed cover, to predict the cover and richness of floral communities, and to investigate the vegetative predictors of monarch abundance. We found significant positive relationships among our YOLO-derived, manually interpreted, and field-measured estimates of milkweed cover. Our manual narrowleaf variables were associated with floral cover and richness, additionally field showy showed an association with floral richness. Moreover, the cover estimates for narrowleaf milkweed (*A. fascicularis*) were predictive of monarch abundance, demonstrating the potential for UAV data combined with machine-learning algorithms to use plant identification to predict habitat characteristics and usage by specialist insects. The high F1 scores from the YOLO models for the Stillwater and Washoe Lake sites also indicated that the YOLO models could be quite accurate. Nevertheless, the F1 scores from Smith Valley were quite low, suggesting that site characteristics are critical to the model's ability to successfully identify plant species that may be quite recognizable in other settings. Interestingly, although all three of our estimation methods for showy milkweed (*A. speciosa*) were highly correlated with one another, none of these estimates were strongly associated with floral community variables or monarch abundance. However, we cannot definitively say that showy area and monarch abundance are not related due to our relatively small sample size for *A. speciosa* in comparison to *A. fascicularis*. Regardless these results suggest that choice of the focal plant species could be critical to reliable estimation of habitat characteristics and associated species.

Our ability to detect plant species with the UAV imagery and machine learning model was heavily influenced by which species we were identifying. In our case, the model could accurately predict the cover of both *A. fascicularis*, and *A. speciosa*, but the phenology and distribution of both species greatly impacted our approach. At all three sites, *A. fascicularis* was abundant, but identification from the orthomosaic images by either manual identification or machine learning required inflorescences. The vegetative qualities of *A. fascicularis* such as its leaves and stems are difficult to separate from the species that surround it, and *A. fascicularis* tended to grow in areas of dense vegetation at our sites. Nevertheless, the inflorescence of *A. fascicularis* is distinctive and easily spotted among species with similar vegetation. Locating *A. speciosa* from the orthomosaic images was easier because it is a large plant with a unique vegetative structure and light green color. The inflorescence of *A. speciosa* stands out in a similar fashion to that of *A. fascicularis*. Interestingly, the inflorescence of *A. fascicularis* persisted for a longer period at our sites, which could potentially impact pollinator preference. Differences in plant architecture affecting UAV identification is a common finding in similar studies. For example, researchers using UAV images to identify two invasive species in Hungarian grasslands found that common milkweed (*Asclepias syriaca*) is easily identified due to its color and structure, whereas blanket flower (*Gaillardia pulchella*) could be identified only by its inflorescence (Bakacsy et al. 2023).

Both of our milkweed species exhibited a strong habitat preference that affected their identification and perhaps even their relationships with monarchs. At our sites, *A. speciosa* is often found in more isolated locations near water sources, further contributing to its ease of identification. For example, at Stillwater, *A. speciosa* was only found growing along the border of the agricultural ditch, whereas *A. fascicularis* was well distributed in the large, grassy field. This does seem to limit the total area that *A. speciosa* can inhabit as it was more sparsely populated than *A. fascicularis* at sites where both species were present, and *A. speciosa* was completely absent from our Washoe site. We observed that *A. fascicularis* seems to be more drought tolerant, as it was often found growing in the drier portions of our sites, which is consistent with prior research (Diethelm et al. 2022). This limited distribution of *A. speciosa* at our sites, and its total absence from one site, severely limited our data for this species, which may have negatively affected our ability to relate this plant species to monarch abundance. The preferred habitat of *A. speciosa* could also potentially limit its distribution across the desert landscape of northern Nevada, negatively impacting its value as a monarch host plant species.

All three of our sites presented unique challenges that influenced data collection in the field, analysis of the orthomosaic images, and the creation of the YOLO models. Smith Valley was the most difficult site to measure both in the field and when analyzing our UAV data. This site spanned the length of an abandoned agricultural ditch where large vegetation was abundant. The milkweeds growing at this site were obstructed by this crowded vegetation and were often found growing beneath or within other plants near the lowest point in the ditch. This made identification from above with our orthomosaic images impossible for the majority of milkweed at this site. The Washoe Lake site had an abundant narrowleaf milkweed population but not a single individual of showy milkweed. This is likely because most of the site lies in a dry grassy field, with the only area near a large water resource being the sandy embankment near the lake, which had a markedly different plant species composition. At Stillwater, we did not find a single monarch larva or egg despite the site having an abundance of both milkweed species and a presence of adult monarchs. This suggests that the presence of milkweed is not the only necessary condition for monarch breeding habitat. One possible explanation for the lack of monarch juveniles at this site could be a high abundance of potential predators, which can be a significant threat to monarch larvae (Diethelm et al. In review). Stillwater seemed to be host to a wide variety of pollinator and predator species, including mantises (Mantodea) mating and laying eggs directly on narrowleaf milkweed plants (G. Zamboni, personal observation).

All three sites were rich in flowering species but identifying floral variables proved to be difficult. Most flowering species at our sites were simply too small to be detected at our image resolution—lower flights producing higher resolution images would be needed for accurate floral identification. Because we could not use the orthomosaic images, we instead used our field measurements of the floral variables along with image segmentation to create predictive random forest models based on the spectral and spatial information of vegetation clusters. The results of these models were marginally correlated with our field variables, but the model strength was impaired by outliers. This was more of an issue for floral cover than it was for floral richness, and in both cases removal of the outliers resulted in a much stronger model. For floral cover, overestimation of this variable in the field may be causing our outlier, as our field measurement is significantly higher than what the model predicted. Despite our difficulties with the field floral variables, floral richness was still associated with monarch count in our penalized regression model. Our correlations revealed that floral cover and richness were marginally associated with our manual narrowleaf measurments, indicating that narrowleaf was a significant floral resource at our sites. There was also a marginal negative association between field showy cover and floral richness, which indicates that showy may be isolated from most floral species. Interestingly, narrowleaf milkweed tended to continue flowering much later in the season than many of the other floral species, and we observed a wide range of pollinating insects visiting the inflorescences. Foral cover and floral richness were also strongly positively correlated. Our results indicate that UAV data with machine learning has potential to estimate floral attributes, but resolution of the images is important. In another similar study, finer scale UAV data (<1 cm) enabled mapping of floral cover and richness, and the relation of those variables to bee abundance and species richness (Torresani et al. 2023). In that study, through several resamples of a given site at varying resolutions, it was discovered that both the accuracy of the floral data and the strength of the relationships between floral and bee variables increased at finer resolutions. This indicates that at high resolutions UAV images and machine learning can predict floral variables directly and their relationships with pollinator species, but that requires a trade-off between the amount of area that can be surveyed in a day and the spatial resolution of the resulting imagery.

Our results also suggest that there may be distinct advantages to UAV-based data collection that may not be reproduced by ground-based data collection methods alone. Our field-measured estimates of both narrowleaf and showy milkweed showed that field-observers consistently overestimated the cover of both species by 13 to 18 times. This is likely due to the oblique view from the ground compared to the overhead view. Furthermore, UAV-based image classification is highly repeatable and accommodates advances in machine learning technology without being subject to interobserver bias. Both narrowleaf and showy milkweed could be readily observed in the UAV imagery with minimal training suggesting that studies could be conducted at larger spatial scales focused solely on milkweed detection. In addition, milkweed patch density may contribute to monarch habitat selection at the landscape scale. Use of landscape metrics derived from patch mapping from UAV imagery is still a relatively new approach that depends on how well the patches can be distinguished from neighboring vegetation types.

We have shown that the area of two common western milkweed species (*A. fascicularis* and *A. speciosa*) can be accurately determined using UAV image data in RGB and a convolutional neural network machine-learning model. This would enable monitoring of these species across large areas with a cost effective, flexible, and easily implemented survey method. These results in combination with field measurements of monarch count allowed us to find a relationship between narrowleaf area and monarch abundance. This demonstrates that our data collection approach can be used to identify relationships between species—even when one of those species is not directly observed in the imagery. The resolution of our images was insufficient for modeling floral cover and richness directly by aerial flower counting. However, field measurements of these floral variables in tandem with image segmentation were used to create floral cover and diversity models that were marginally correlated with our field floral variables. Our study demonstrates the utility of both UAV imagery and machine learning models across sites with diverse plant communities for mapping two species of milkweed and understanding plant-pollinator relationship for one of the most iconic species in North America.

## CHAPTER 5: UAV Study Figures and Tables

**Table 1**. The dates for each field outing, along with details on which dates manual surveys and UAV surveys took place.

| Date | Manual survey? | UAV survey? |
|---|---|---|
| 20-Jun-23 | YES | YES |
| 5-Jul-23 | YES | NO |
| 25-Jul-23 | YES | YES |
| 11-Aug-23 | YES | NO |
| 29-Aug-23 | YES | YES |
| 20-Sep-23 | YES | NO |
| 4-Oct-23 | YES | NO |

**Table 2**. The correlation coefficient of each relationship is displayed here. Correlations for which the Bonferroni correlation is significant are given one asterisk (*); and relationships for which P < 0.05 are in bold.

| | Field Narrowleaf Cover (%) | Field Showy Cover (%) | Field Floral Cover (%) | Field Floral Richness (%) | Manual Narrowleaf Cover ($m^2$) | Manual Showy Cover ($m^2$) | YOLO Narrowleaf Cover ($m^2$) | YOLO Showy Cover ($m^2$) |
|---|---|---|---|---|---|---|---|---|
| Field Narrowleaf Cover (%) | 1 | | | | | | | |
| Field Showy Cover (%) | 0.115 | 1 | | | | | | |
| Field Floral Cover (%) | 0.093 | -0.108 | 1 | | | | | |
| Field Floral Richness (%) | 0.073 | **-0.201** | **0.613*** | 1 | | | | |
| Manual Narrowleaf Cover ($m^2$) | **0.745*** | 0.057 | **0.237** | **0.196** | 1 | | | |
| Manual Showy Cover ($m^2$) | 0.127 | **0.789*** | -0.087 | -0.098 | 0.048 | 1 | | |
| YOLO Narrowleaf Cover ($m^2$) | **0.704*** | 0.024 | 0.137 | 0.136 | **0.926*** | 0.037 | 1 | |
| YOLO Showy Cover ($m^2$) | 0.075 | **0.632*** | 0.006 | 0.017 | 0.060 | **0.802*** | 0.033 | 1 |

**Table 3**. Performance of the YOLO predictions of milkweed cover compared to manual identification of milkweeds from the orthomosaic images. True and false positive are proportions (%) of the total YOLO output and false negative is a proportion of the total ground truth. The F1 score indicates the harmonic mean of the precision and recall of the YOLO model; cases where the F1 score is above 0.7 are in bold.

| | True Positive | False Positive | False Negative | F1 Score |
|---|---|---|---|---|
| Stillwater Showy | 56.812 | 43.505 | 5.397 | **0.712** |
| Stillwater Narrowleaf | 80.363 | 19.637 | 7.818 | **0.863** |
| Washoe Narrowleaf | 82.522 | 17.478 | 27.883 | **0.803** |
| Smith Valley Showy | 6.745 | 93.257 | 51.669 | 0.113 |
| Smith Valley Narrowleaf | 1.114 | 98.886 | 54.56 | 0.021 |

**Table 4**. Associations between landscape metrics and monarch abundance. Relationships for which P < 0.05 are in bold.

| | Estimate | Standard Error | Z-Value | R-Squared | P-Value |
|---|---|---|---|---|---|
| Showy shape index (Mean) | -0.050 | 0.598 | -0.083 | 0.019 | 0.934 |
| Showy shape index (Standard deviation) | -31.769 | 55.400 | -0.573 | 0.020 | 0.566 |
| Showy Euclidean nearest neighbor (Mean) | -0.0003 | 0.013 | -0.022 | 0.019 | 0.983 |
| Showy Euclidean nearest neighbor (Standard deviation) | -0.035 | 0.591 | -0.059 | 0.019 | 0.953 |
| Average Distance to neighboring showy patches within 5 m (Mean) | -0.186 | 0.123 | -1.513 | 0.039 | 0.130 |
| Narrowleaf shape index (Mean) | 1.088 | 0.415 | 2.623 | 0.043 | **0.009** |
| Narrowleaf shape index (Standard deviation) | 8.36 | 10.730 | 0.779 | 0.022 | 0.436 |
| Narrowleaf Euclidian nearest neighbor (Standard Deviation) | 1.031 | 0.496 | 2.077 | 0.040 | **0.038** |
| Narrowleaf Euclidean nearest neighbor (Mean) | -0.026 | 0.009 | -2.925 | 0.049 | **0.004** |
| Average distance to neighboring narrowleaf patches within 5 m (Mean) | -0.384 | 0.100 | -3.845 | 0.080 | **0.0001** |

**Figure 1**

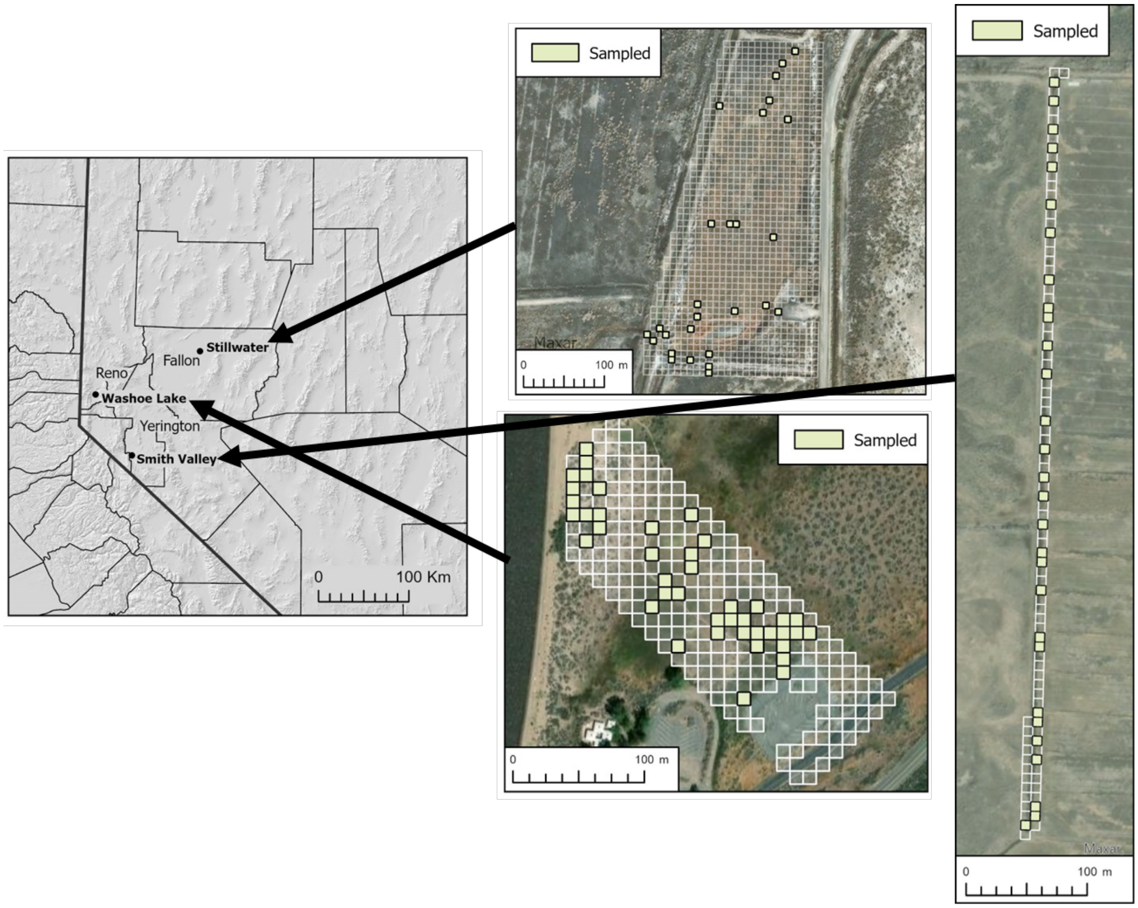


Locations of survey sites in northern Nevada and maps of each site showing all 10x10 meter plots with sampled plots highlighted.

**Figure 2**

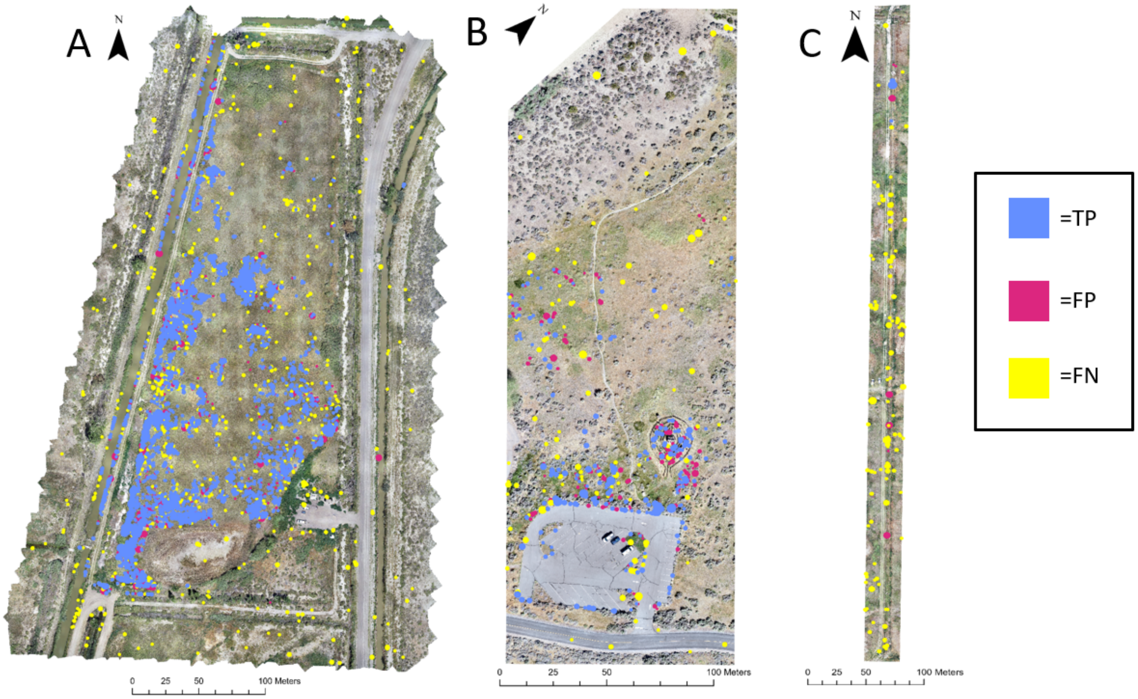


Orthomosaic maps of narrowleaf milkweed at Stillwater (left), Washoe Lake (Center), and Smith Valley (Right). The true positives (yellow), false positives (orange), and false negatives (red) from the YOLO model are identified by color and the size of the polygons scale with the size the milkweed patch they are representing.

**Figure 3**

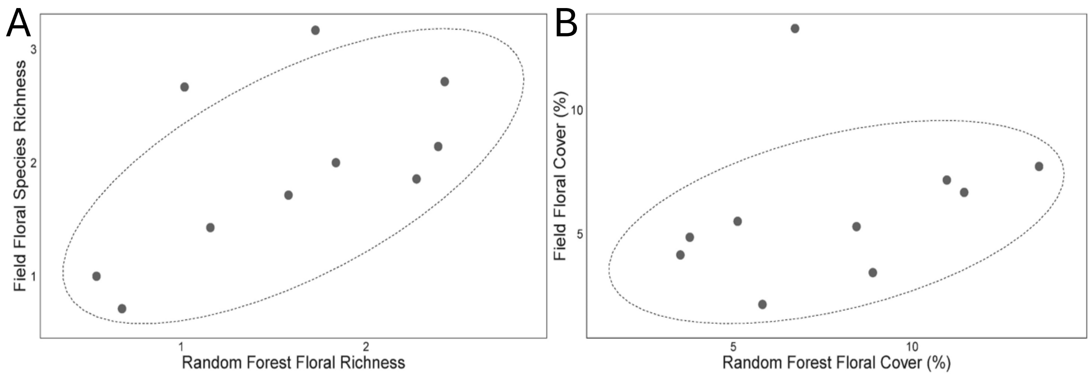


These plots show the field values for floral cover (left) against the random forest predicted values, and the field values for floral richness (right) against the random forest predicted values. The ellipses represent an 80% confidence interval.

**Figure 4**

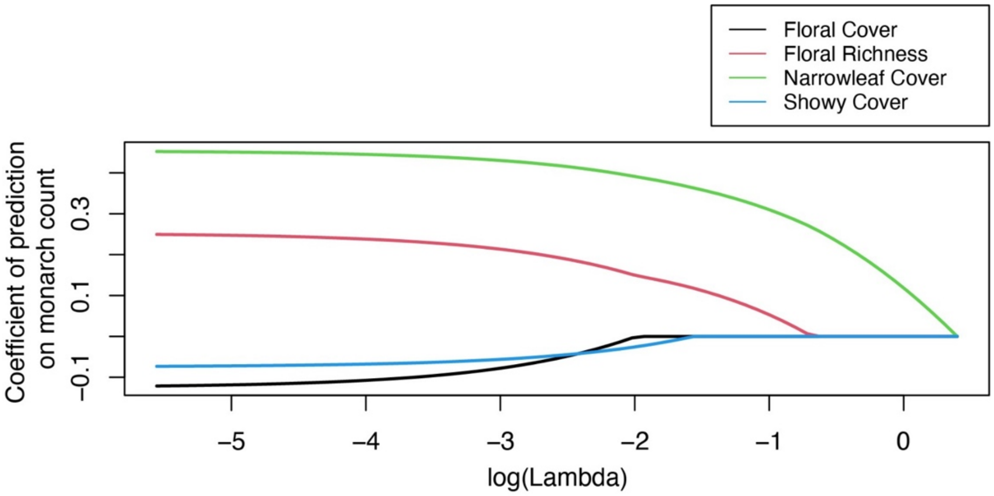


Coefficient paths from the elastic-net regularized regression model showing how floral cover, floral species richness, and milkweed abundance (as summarized by principal components) predict monarch abundance across a range of penalty values (log lambda).

**Figure 5**

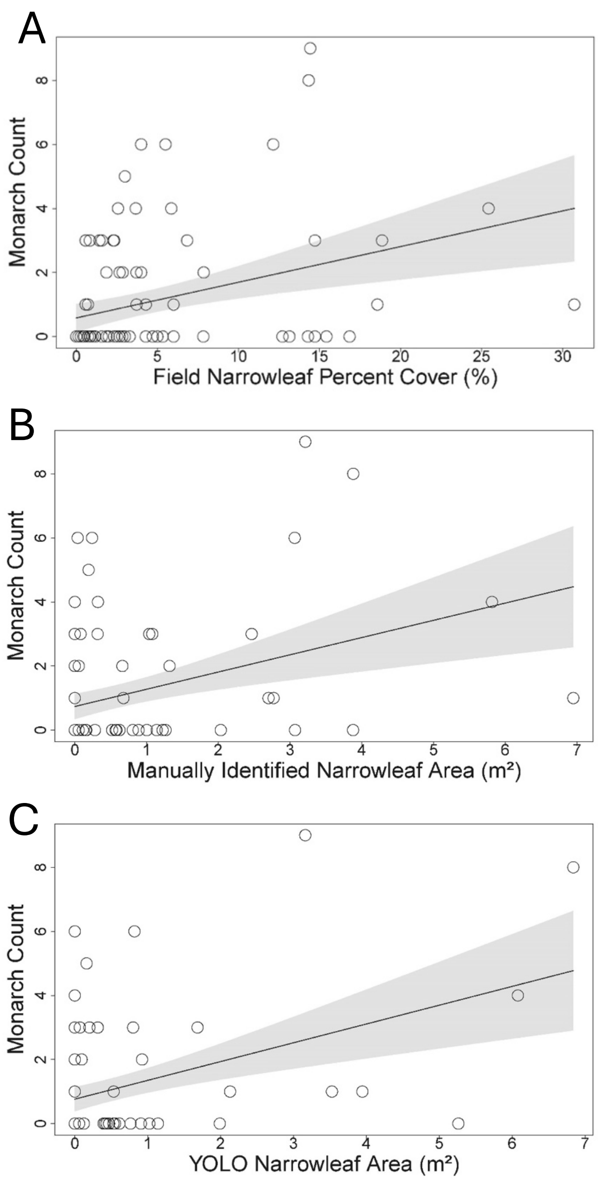


These plots show the association between monarch counts and field narrowleaf cover (top), human-interpreted narrowleaf area (middle), and YOLO narrowleaf area (bottom).

**CHAPTER 6: Roadviewer Study Background**

Understanding the spatial pattern of plant distributions on Earth is a major goal in ecology, and a first step towards understanding how abiotic factors control and shape distributions is to accurately map species occurrences. Species distribution models (also known as habitat suitability models, ecological niche models, or climatic envelope models) are one of the most common approaches to understanding how abiotic and landscape factors control the occurrence of organisms. Special challenges exist when it comes to commonly occurring, disturbance-mediated, or anthropogenic-associated organisms. The most common approach for describing the location of organisms in a species distribution model involves contrasting known locations (presences) against randomly chosen background locations that characterize the environment available to the organism. Past approaches using systematic field surveys, museum records, and citizen-science have resulted in larger occurrence databases and more robust models. However, the use of street-level photography has been relatively unexplored.

Street-level photography has the potential to offer enormous progress in species distribution modeling because of the large number of photographs, lack of bias that may occur because of the distributed nature of sampling, and ability to sample evenly across areas in which commonly occurring and anthropogenic-associated species exist. Street-level photography offers advantages that are inherent to other remote sensing approaches, namely that they are repeatable unlike field surveys. The large number of photographs derived from such an approach can be analyzed post-hoc allowing for improvements in the machine learning to potentially improve classification accuracy through time. Repeat sampling using street-level photography has the potential to reduce inter-observer bias, including bias with regards to taxonomic identification. Despite the potential that street-level photography offers for ecology there remain many obstacles that have not been adequately explored. The ability to correctly identify and count individual plants may depend on the specific study area, as well as on the plant architecture, time of year, and visual contrast between the focal plant species and other species in the vicinity.

Milkweeds (genus *Asclepias*) are the host plant for the monarch butterfly (*Danaus plexippus*), which has declined by 97% in western North America (Pelton et al. 2019). Although the declines in monarch populations are likely driven by several factors (Pleasants and Oberhauser 2013; Crone et al. 2019), loss of milkweeds over time may be one contributing factor in monarch decline. Improving the tracking and monitoring of both milkweed and monarch populations through time is a major objective in monarch conservation (Cariveau et al. 2019). Within North America the monarch butterfly population is frequently divided into an eastern population, which overwinters in Mexico and a western population, which overwinters along the California coast. A previous study using citizen-science, museum records, and agency databases developed predictive models of habitat suitability for the western population of the monarch butterfly and thirteen species of milkweed host plants for seven western states (California, Oregon, Washington, Idaho, Nevada, Utah, and Arizona) (Dilts et al. 2019). These habitat models have been used by land management agencies to prioritize habitat management through State Wildlife Action Plans (Harris et al. 2023). However, predictive maps derived from correlative modeling approaches result in predictions of potential habitat suitability (i.e. potential niche) which may or may not coincide with true habitat suitability (i.e. realized niche). Remote sensing approaches to mapping species occurrences, such as the use of street-level photography, has the potential to develop more complete inventories for all sampled areas.

Street-level photography has been applied in a limited number of cases for mapping important species that contribute to ecological services. In one example, Seiferling et al. (2017) used Google Street View imagery to map urban canopy cover in both New York City and Boston. They argue that street-level imagery may correspond with perceived canopy cover and augment, rather than replace, existing mapping methods for urban canopy cover, such as

LiDAR and high-resolution aerial photography. Street-level photography and artificial intelligence have been used to map *Asclepias syriaca* (common milkweed) along roadsides in two counties in Iowa (Ozcan et al. 2020). Although this species of milkweed is not present in western North America it is visually similar to showy milkweed, which is one of the most common milkweed species in the western U.S. However, Ozcan et al. (2020) did not test their approach on other milkweed species, which may be more difficult to identify. In difficult classification cases image augmentation techniques have been valuable at improving classification accuracy (Shorten and Khoshgoftaar 2019). Image augmentation works by randomizing the training imagery to reduce model overfit and improve the generalizability of models (Shorten and Khoshgoftaar 2019). For example, lighting conditions can be artificially increased or decreased and the location of the objects within the image can be randomized. We know of no published studies that have that have used image augmentation to improve the classification accuracy of milkweeds from street-level photography.

In the study we tested an approach to mapping the distribution of two *Asclepias* species; *A. speciosa* (showy milkweed) and *A. fascicularis* (narrowleaf milkweed), the two most common milkweeds in the western United States, using street-level photography in three agricultural valleys in northern Nevada, U.S.A. The two milkweed species offer two endpoints in expected classification accuracy. We predicted that it would be easier to classify showy milkweed than narrowleaf milkweed due to its wide leaves, large distinctive flowers, and light color. In contrast, narrowleaf milkweed has narrow leaves, white/yellow flowers, and a more typical green color making it likely more difficult to distinguish from other vegetation. We ask the following questions:

1) Can street-level photography and machine learning be used to accurately classify each of the two species of milkweed?

2) What are the conditions needed to allow for street-level photography and machine learning to successfully classify milkweeds?

3) Can image augmentation improve the classification accuracy for species, such as narrowleaf milkweed, that visually resemble other species in the photographs?

The results of our study are broadly applicable because they help us understand the conditions under which the use of street-level photography for species occurrence mapping is likely to be successful for two contrasting, yet ecologically important species. The maps derived from this study offer the potential to develop roadside prescriptions, such as mowing and herbicide applications, which are critical for human safety, fire prevention, and noxious weed management while also providing habitat for the monarch butterfly.

## CHAPTER 7: Roadviewer Study Research Approach

Our study area encompasses three agricultural valleys (Lahontan, Mason, and Carson) in northern Nevada, U.S.A. (Figure 6). These three valleys have some of the largest populations of showy and narrowleaf milkweed in the state of Nevada, as indicated in the predictive maps of Dilts et al. (2019) and citizen-science databases such as the Western Monarch and Milkweed Mapper (Xerces Society 2018). Although more than a dozen milkweed species are found in the state of Nevada, we limited the study to include only showy and narrowleaf milkweeds because they are the two most common species and tend to occur along roadsides (Dilts et al. 2019; Pelton 2018). Both species are known to commonly occur in areas with elevated moisture levels, including alongside diches, roadsides, pastures, and agricultural fields.

Our study makes use of the Nevada Department of Transportation RoadViewer dataset, which was originally developed for assessing pavement conditions. The RoadViewer database utilized in this study was collected using an instrumented vehicle equipped with a high-resolution side-view camera. The camera features a 50-degree Field of View (FOV) and is mounted at a 54-degree angle from the vertical axis of the vehicle's direction. This setup was designed to capture detailed images of roadside vegetation. The database comprises 64 data collection sessions (ranging from October 2017 to September 2022) conducted along all NDOT-managed highways in the three study areas. Thus, while being a spatially extensive dataset RoadViewer does not represent a complete inventory of all roads within our study area. We also explored but chose not to use Google StreetView imagery because of its grainy nature and poor lighting conditions in these rural areas. Each session captured a series of consecutive trajectory points at a 1-second frequency, each linked to a corresponding side-view image. To ensure high-quality data, the driver of the instrumented vehicle maintained a consistent between 8 and 8.1 m/s (17.9 – 18.2 mph), optimizing the capture of detailed roadside imagery. Each image is georeferenced, and geolocations and image names are attached to a point shapefile in a Geographic Information System (GIS). Images are taken in both the forward and right-facing directions for all Nevada Department of Transportation managed highways covering 386 km of roadway, although only right-facing images were used in this analysis. The dataset includes a total of 157,333 images, each with a resolution of 2448 x 2050 pixels.

To create model training, validation, and testing data we visually assessed 2,225 images, of which 650 contained showy milkweed, 245 contained narrowleaf milkweed, 99 contained both species, and the remaining 1,231 contained no milkweed (Table 5). Milkweeds are relatively rare in this landscape so we opted to use a stratified random sampling approach based on a previously published habitat model. Using the maps from Dilts et al. (2019) we extracted 270-meter predicted habitat suitability that intersected Nevada Department of Transportation managed roads. We split the maps into 10 equal-area (decile) classes and randomly selected an equal number of images from each decile. Manual identification and labeling of milkweeds in images was done using the online software RoboFlow 3.0 (RoboFlow 2024) by one of the authors (GZ), who had good knowledge of milkweed biology and the study area. Patches of milkweeds were delineated as bounding boxes. In cases in which milkweeds occurred in continuous clusters these were delineated using a single bounding box. In other instances, bounding boxes might only represent a single individual. We did not apply a distance cut-off but rather sought to delineate each milkweed that was visible in the image no matter the location. Bounding boxes thus included both the road right-of-way and adjacent properties. The resulting dataset included 3656 number of bounding boxes for showy and 1588 number of bounding boxes for narrowleaf milkweed.

The entire dataset was split into 70% for model training, 20% for validation, and 10% for testing. The training split provides annotated milkweed visual features for the applied computer vision model to build its internal parameters. The validation split is created to evaluate the model during training process to prevent the overfitting phenomenon (Ali and Zhang 2024), and the testing split gives the final performance evaluation.

Following the creation of the dataset, the training set was expanded using image augmentation techniques to enhance the model's robustness and increase the diversity on conditions of training data. The primary focus of these augmentations was adjustment of lighting conditions, which are influenced by variation in weather during data collection by the instrumented car. A random brightness adjustment factor, ranging from -15% to +15%, was applied to each image to simulate different lighting scenarios. Additionally, blur and noise augmentations were implemented to improve the model's ability to detect milkweed instances at farther distances. After applying these augmentation techniques, the images were randomly sampled and clipped to form the post-augmented training set, which included a total of 2,538 images.

Deep learning models utilized in computer vision, particularly for image processing, typically derive from Convolutional Neural Networks (CNNs). These models use convolutional filters to extract features from images and accurately identify objects within them. Object Detection models identify specific objects within an image, pinpointing their locations with bounding boxes and providing associated category labels. Given the extensive RoadViewer data collected across Nevada, the YOLO (You Only Look Once) model version 8.0 (Redmon 2016), a state-of-the-art Object Detection framework, was chosen for this task. YOLO employs a CNN backbone to learn hierarchical image features in a single-stage process, predicting the bounding boxes and corresponding confidence levels (ranging from 0 to 1) of detected objects.

The YOLOv8 is trained through a complied dataset as described previously using the training split in an iterative process. In each iterative epoch, the parameters in the neural network are adjusted accordingly based on the visual features in the training images and corresponding bounding box annotations, which elaborates a backward propagation. In the end of training process, the well-trained convolutional filters would be more activated to the visual features indicated by the annotations over other instances and thereby providing accurate object detection.

In the model evaluation, the validation and testing split consisting of 30% of the study images that were not used in model training, are used to reveal the performance of trained model. The evaluation is conducted at the image-level instead of the individual object level (the bounding boxes) within images. The detection performance of two species are evaluated separately using following definitions in terms of evaluation metrics:

Positive Image: A street-level image with at minimum one detected milkweed objects over a confidence threshold.
Negative Image: A street-level image with no detected milkweed object over a confidence threshold.

Based on which, following evaluation metrics are defined:

True Positive (TP): The street-level images contain milkweed, and the model reported at minimum one milkweed object;
False Positive (FP): The street-level images without milkweed, while the model reported at minimum one milkweed object;
True Negative (TN): The street-level images without milkweed, and the model reported no milkweed object;
False Negative (FN): The street-level images contain milkweed, while and the model reported no milkweed object;
Precision: the precision elaborates a metric ranges from 0 to 1, higher precision indicates more correctly reported images among those positive images, the

$$Precision = \frac{TP}{TP + FP}$$

Recall: the recall, on the other hand, explains the portion of images that are actually positive, are reported positive by the model

$$Recall = \frac{TP}{TP + FN}$$

F1-Score: The F1-Score is one of the most commonly used measures in machine learning for evaluating a confusion matrix and is calculated as the harmonic mean of precision and recall (Pillai et al. 2017). A higher F1 reflects better overall performance.

$$F1 = \frac{2 \times Precision \times Recall}{Precision + Recall}$$

The classification accuracy and F1-Score were evaluated across varying confidence thresholds, which helps to identify the best confidence threshold for identifying the milkweed of both milkweed species.

We assessed the effects of image augmentation for improving model accuracy for both showy and narrowleaf milkweed by calculating precision, recall, and the F1-Score comparing models derived using image augmentation to a base model using no image augmentation. We also assessed the influence of the area of prediction bounding boxes (a rough proxy for the density of milkweed) on model accuracy using a Sum Area Ratio: the sum of all predicted milkweed bounding boxes within an image divided by the total area of the image. We also measure how precision, recall, and the F1-Score differ between models in which bounding box size is used as a filter to reduce the number of false positives.

## CHAPTER 8: Roadviewer Study Findings and Applications

The models predicting showy and narrowleaf presence from RoadViewer images had high overall accuracy (95 and 93%), high precision (95 and 91%), and a relatively high $F_1$ score (93 and 86%). Recall was lower for narrowleaf milkwed (81%) than for showy milkweed (90%). These results indicate that models predicting the presence of showy milkweed had higher overall accuracy and a lower percentage of false positives and false negatives than the models for narrowleaf milkweed.

The optimal threshold for classifying images as evaluated by the F1-score was 0.5 for showy and 0.3 for narrowleaf milkweed (Figure 7). The curve for showy milkweed showed a unimodal shape with a single peak suggesting that the tradeoff between false negatives and false positives was fairly straightforward. In contrast, narrowleaf showed a lower overall $F_1$ and its curve was broader suggesting that the choice of a threshold between 0.3 to 0.65 could result in a tradeoff with a lower threshold resulting in more false positives (milkweed that are detected but not true milkweed) and a higher threshold resulting in more false negatives (failure to detect a true milkweed).

Models derived using image augmentation outperformed base models without image augmentation for both milkweed species, and the improvement in model performance was consistent across all metrics that we analyzed. For showy milkweed the $F_1$ score increased from 0.65 to 0.93, precision improved from 0.70 to 0.95, and recall improved from 0.61 to 0.90 (Table 6). For narrowleaf milkweed the $F_1$ score increased from 0.59 to 0.86, precision improved from 0.64 to 0.91, and recall improved from 0.55 to 0.81 (Table 6). Although showy milkweed had higher accuracy by all measures image augmentation appears to have had a larger impact on narrowleaf accuracy compared to base models (Figure 8).

Post-processing techniques, such as filtering by the total area of prediction bounding boxes, improved model accuracy for both showy and narrowleaf milkweed. We determined that 0.5% as the optimal total area of prediction bounding boxes. Images that had less than 0.5% were more likely to contain false positives (Figure 9). Post-processing had a larger impact on models predicting narrowleaf occurrences than on models predicting showy occurrences (Figure 10).

We further examined the types of misclassification by selecting a subset of 90 images and examined which species/object the milkweed was misclassified. Narrowleaf milkweed was the more commonly misidentified species of the two milkweeds, which is consistent with it having a morphology (narrow leaves, less glaucous, and smaller flowers compared to showy) that is more similar to other vegetation types within the study areas (Figure 11). The objects that were most commonly misidentified were other plant species with the most common being rubber rabbitbrush (n=14), cottonwood (n=6), forage kochia (n=5), bitterbrush (n=4), gumweed (n=4), sagebrush (n=3), and tall whitetop (n=2). Non-vegetative misidentification included light soil (n=3), white plastic litter (n=2), and clouds (n=1). A large number of misclassifications were not identifiable to our visual interpreter (GZ).

Both species of milkweed were relatively rare within our study area (Figure 12), with only 5.7% of images containing showy milkweed and 1.4% containing narrowleaf resulting in 7564 and 1915 images respectively (Table 7). Using the 250x250 meter grid the percentage of the landscape predicted to contain at least one narrowleaf milkweed occurrence ranged from 21% in Mason Valley to 46% in Lahontan Valley with an average across all three valleys of 39% (Table 7). Showy milkweed was predicted to be more common on the landscape occupying 70% of grids and ranging from 63% in Mason Valley to 84% in Carson Valley. The average number of narrowleaf predictions per grid ranged from 0.49 in Mason Valley to 1.67 in Lahontan Valley. For showy the averages ranged from 3.0 in Mason Valley to 5.6 in Lahontan Valley (Table 7).

## CHAPTER 9: Roadviewer Study Conclusions and Suggested Research

In this study we use street-level imagery (RoadViewer) collected by a public transportation management agency (Nevada Department of Transportation) and an artificial intelligence model (YOLO) to automate the mapping of two species of milkweed (*Asclepias speciosa* (showy) and *Asclepias fascicularis* (narrowleaf)) critical to the life cycle of the monarch butterfly (*Danaus plexippus*). The original purpose of the RoadViewer imagery by the Nevada Department of Transportation is not for species mapping, but rather, to identify areas in which pavement maintenance and rehabilitation is needed. Hence, the use of the street-level imagery for ecological purposes can be viewed as a low-cost approach that achieves the goals of roadside conservation while at the same time being consistent with other goals of the transportation agency (e.g. pavement management). Our results indicate that without image augmentation and post-processing we were able to detect showy and narrowleaf milkweed, but at accuracy levels that are lower than what might be typically desirable ($F_1$ scores of 0.65 and 0.59 for showy and narrowleaf, respectively). The lower level of accuracy for narrowleaf compared to showy was expected because the morphology and the phenology of showy tends to be more distinct from other plants compared to narrowleaf. For example, rubber rabbitbrush (*Ericameraia nauseosa*), tall whitetop (*Lepidium latifolium*), and yellow toadflax (*Linaria vulgaris*) are all more common in our study area than narrowleaf milkweed and have flowers that can be confused with narrowleaf milkeed. Without image augmentation or post-processing the results of these models may still be useful in identifying areas suitable for manual review of imagery and field validation resulting in time savings compared to traditional field surveys.

Both image augmentation and post-processing filtering proved successful in improving accuracy for both milkweed species, increasing the $F_1$ score to 0.93 and 0.86 for showy and narrowleaf milkweed. Image augmentation is a technique that has gained widespread use in deep learning (Shorten and Khoshgoftaar 2019) and is increasingly being used in ecology for tasks such as wildlife detection from camera traps, satellite and airborne remote sensing, and enhanced use of citizen science through uploaded photographs (Christin et al. 2019; Bothmann et al. 2023; Rillig et al. 2024). Image augmentation techniques, such as rotating and flipping images, and adjusting contrast appear to reduce overfitting in image classification by increasing the kinds and situations in which the object is present (Shorten and Khoshgoftaar 2019). In our study area, photographs taken of a road in which milkweeds were abundant during overcast conditions appears to have biased the model without image augmentation. Rotating and flipping images appears to have increased the ability of the model to identify far-away instances of milkweeds. The efficacy of image augmentation in increasing classification accuracy is likely dependent on the particular application with ones in which overfitting is likely to be an issue to be the strongest candidates for image augmentation techniques. In our case, classification accuracy of both species improved by image augmentation, but improvements were more pronounced for narrowleaf, likely because it was the harder-to-classify species.

Post-processing also improved the accuracy of our models, particularly for narrowleaf milkweed, which tended to resemble other plant species. Our post-processing technique was relatively simple. Images in which the overall area occupied by bounding boxes of milkweed predictions was less than 0.5% (half of one percent) were removed as occurrences and treated as absences. This had the effect of removing low-probability noisy classification results. Post-processing techniques are not limited to describing the overall area of the image classified, but can also describe the number, size, shape, and arrangement of objects within an image. Post-processing has a history of use in the medical imaging fields (Salvi et al. 2021) and in remote sensing where it has been used to improve the readability and aesthetic qualities of maps

(Seebach et al. 2013). Software for calculating landscape metrics, such as FRAGSTATS (McGarigal 2015) or the landscapemetrics package in R (Hesselbarth et al. 2019), could be used in post-processing to improve image classification.

Our study is one of a very small number that uses vehicle-mounted repeat photography to map roadside milkweeds and possibly the first in the western United States. Ozcan et al. (2020) used a similar hood-mounted camera system and Faster R-CNN (region-based convolutional neural network) to map common milkweed (*Asclepias syriaca*) using 2,746 images in central Iowa. Our study was larger (157,333 images) and used an existing system by the Nevada Department of Transportation that spanned six years ranging from May to October. Our study also appears to be the first to compare image augmentation and post-processing techniques for improving roadside milkweed classification accuracy. Our results indicate that image augmentation may be critical for improving classification accuracy, even for difficult to classify species such as narrowleaf milkweed. Common milkweed (*Asclepias syriaca*) is much more similar morphologically to showy milkweed as it has broad leaves, large flowers, and lighter-colored leaves. Although comparisons across species and geography is challenging and needs to be interpreted with caution, our results show similar levels of accuracy to Ozcan et al. (2020) without image augmentation and post-processing and higher levels using these two approaches.

The use of street-level photography in ecology is growing although the applications of these data have mostly been limited to a few scenarios. The most common applications of street-level appears to be for mapping urban street trees (Seiferling et al. 2017; Stubbings et al. 2019; Laumer et al. 2020; Lumnitz et al. 2021) followed by crop type and phenology mapping (d'Andrimont et al. 2018; Yan et al. 2021; Liu et al. 2024), and invasive species mapping (Pardo-Primoy and Fagúndez 2019; Kotowska et al. 2021; Ulus et al. 2021). Studies using street-level imagery for mapping rare species, threatened and endangered species, and important wildlife species are few, as are studies quantifying pollinator resources (but see Burr et al. 2018; Murphy and Crone 2025). With the availability of commercial datasets, such as Google StreetView, Microsoft Streetside, and the ability for agencies, universities, and individuals to create their own hood-mounted camera systems, combined with advances in artificial intelligence we anticipate that the availability of street-level photography will rapidly increase and that databases generated from these approaches will greatly augment field-based data collection. Further, roadside mapping using these approaches can guide future field sampling potentially leading to increases in sampling efficiency and reproducibility.

Although our study used many images across a wide variety of conditions, we caution against using these models to predict milkweed occurrences outside the range of the training data. Expanding the geographic scope of the study would likely result in more species with similar morphologies and phenologies to the two milkweed species that we examined, which would reduce classification accuracy without more training. Another challenge that we encountered had to do with the number of years and seasonal images that we included in the RoadViewer database. We believe that better accuracy may be achieved by reducing the number of months to avoid confusion between milkweed and other plants. For example, collecting RoadViewer imagery in July might avoid the flowering season for rubber rabbitbrush, which tends to flower in August and September and is extremely common throughout the study area. Although the purpose of our study wasn't to track changes in milkweed abundance through time, street-level imagery, if collected in the same areas at the same phenological stage, might be valuable for monitoring.

Roadsides are among the most ubiquitous, visible, and actively managed habitat for monarch butterflies (Kasten et al. 2016). Properly timed mowing has the potential to increase young milkweed and promote monarch butterfly habitat. In a study of experimental and control plots in southern Ontario Knight et al. (2019) found that properly timed mowing increased the number of eggs found in roadside plots. In their study, located at 43°N, mowing was most effective between the 2nd and 3rd weeks of July after which mowing likely resulted in monarch mortality. Use of mowing as a strategic management tool will likely require local studies on specific species. In the western U.S. showy and narrowleaf are the two most common roadside milkweed species. Herbicides are another management tool commonly applied to reducing weeds and enhancing motorist visibility along side roadways. Herbicides have increasingly been identified as a potential major cause of milkweed loss in the agricultural midwestern United States (Pleasants and Oberhauser 2013). By repeat surveying historical records Lalonde et al. (2022) concluded that occurrences of roadside milkweeds in southern Quebec and Ontario are 33 to 86% lower than in 1943 and 1944 and found that their indicators of mowing did not explain the decline. They suggest that herbicide applications may have resulted in these declines. Halsch et al. (2020) found high levels of pesticides (insecticides, fungicides, and herbicides) on plants across northern California, including some plants sold at nurseries for home gardeners. Although more research is needed on the roadside application of herbicides and pesticides on both milkweeds and monarchs we advocate precaution in the use of herbicide on roadside milkweeds. Mapping roadside milkweeds using street-level imagery provides managers with relevant data from which to make targeted management decisions.

Given the importance of milkweeds in the life cycle of the monarch butterfly accurate mapping of milkweed distributions and abundance is critical for understanding its distribution on the landscape and enhancing conservation opportunities. Roadside management has been viewed as one of the key strategies towards enhancing breeding habitat for monarch butterflies (Kasten et al. 2016; Cariveau et al. 2024). Techniques that apply a limited number of field samples to develop statistical models and predict potential occurrence of milkweeds on the landscape may suffer from the fact that potential habitat may not always be occupied for a number of reasons (competition, predation, disease, disturbance). Street-level imagery offers a promising new approach for mapping the actual distribution of milkweeds and may enhance our understanding of how population processes relate to landscape factors.

Our study greatly expands the scope of street-level automated mapping of milkweeds and illustrates that image augmentation and post-processing may prove valuable for increasing the accuracy, particularly for species, such as narrowleaf milkweed, that are difficult to predict. Automated maps of milkweed occurrence can be used to guide roadside management (particularly mowing and herbicide application), enhance species distribution models, and guide further field surveys.

## CHAPTER 10: Roadviewer Study Tables and Figures

**Table 5**: Number of images used to train, validate, and test models based on manual human interpretation.

| Training set (70%) | | | |
|---|---|---|---|
| **Narrowleaf** | **Showy** | **Both** | **Empty** |
| 185 | 484 | 66 | 862 |
| **Validation and testing set (30%)** | | | |
| **Narrowleaf** | **Showy** | **Both** | **Empty** |
| 60 | 166 | 33 | 369 |

**Table 6**: Accuracy statistics for the presence-absence models of showy and narrowleaf milkweed showing precision, recall, and the $F_1$ statistic for models using image augmentation (upper) and models that do not use image augmentation (lower). Thresholds used for delineating milkweed from non-milkweed detections were 0.5 and 0.3 for showy and narrowleaf milkweed in the model that used augmentation and 0.4 and 0.45 for showy and narrowleaf in the base model that did not include augmentation.

| | | | | |
|---|---|---|---|---|
| **Showy (0.5)** | **TP** | **FN** | **FP** | **TN** |
| | 179 | 20 | 9 | 816 |
| | **Precision** | **Recall** | **F1-score** | |
| | 0.95 | 0.9 | 0.93 | |
| **Narrowleaf (0.3)** | **TP** | **FN** | **FP** | **TN** |
| | 75 | 18 | 7 | 924 |
| | **Precision** | **Recall** | **F1-score** | |
| | 0.91 | 0.81 | 0.86 | |

| | | | | |
|---|---|---|---|---|
| **Showy (0.4)** | **TP** | **FN** | **FP** | **TN** |
| | 122 | 77 | 52 | 773 |
| | **Precision** | **Recall** | **F1-score** | |
| | 0.70 | 0.61 | 0.65 | |
| **Narrowleaf (0.45)** | **TP** | **FN** | **FP** | **TN** |
| | 51 | 42 | 29 | 902 |
| | **Precision** | **Recall** | **F1-score** | |
| | 0.64 | 0.55 | 0.59 | |

**Table 7**: Milkweed prediction statistics for each species (narrowleaf and showy) in each of the three study valleys (Carson, Mason, and Lahontan). The average number of narrowleaf and showy occurrences in a 250x250 meter cell as predicted by the YOLO model. The total number of Roadviewer images expected to contain narrowleaf and showy milkweed in each of the three valleys. The total number of 250x250 meter cells with at least one predicted occurrence of milkweed for each valley. The grids column shows the number of 250x250 meter boxes per valley. The frames column shows the number of photographs per 250x250 meter grid.

| | Narrowleaf average | Showy | Narrowleaf sum | Showy | Narrowleaf non-zero | Showy | Grids | Frames |
|---|---|---|---|---|---|---|---|---|
| Carson | 0.85 | 4.6 | 312 | 1,671 | 146 | 308 | 365 | 19,665 |
| Mason | 0.49 | 3.0 | 191 | 1,142 | 82 | 244 | 386 | 21,759 |
| Lahontan | 1.67 | 5.6 | 1,412 | 4,751 | 396 | 567 | 846 | 89,475 |

**Figure 6**

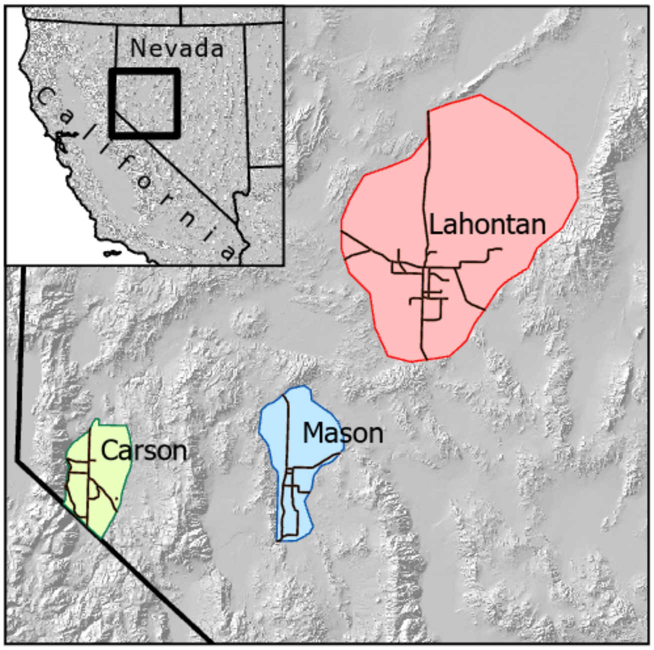


Map showing the location of the three study areas. State of Nevada Department of Transportation (NDOT) managed roads are shown as black lines in each of the three valleys (Carson, Mason, and Lahontan).

**Figure 7**

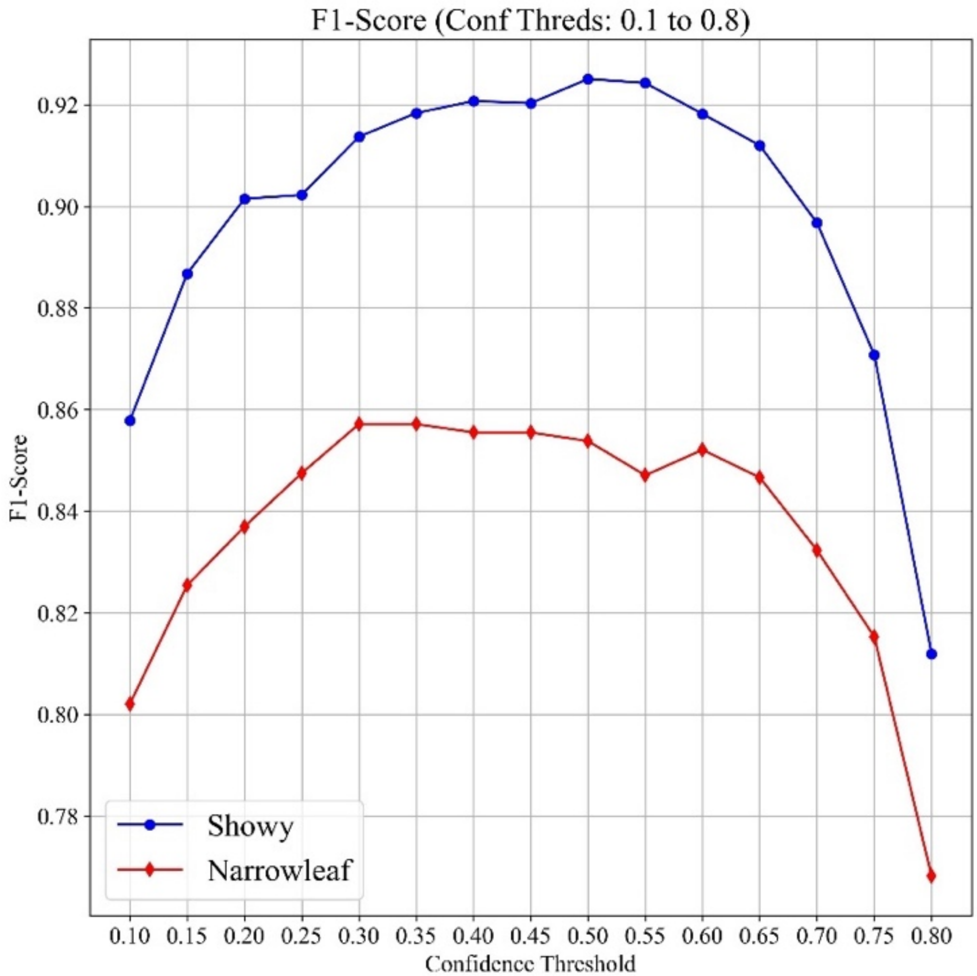


$F_1$ scores used to optimize threshold selection for showy and narrowleaf models.

**Figure 8**

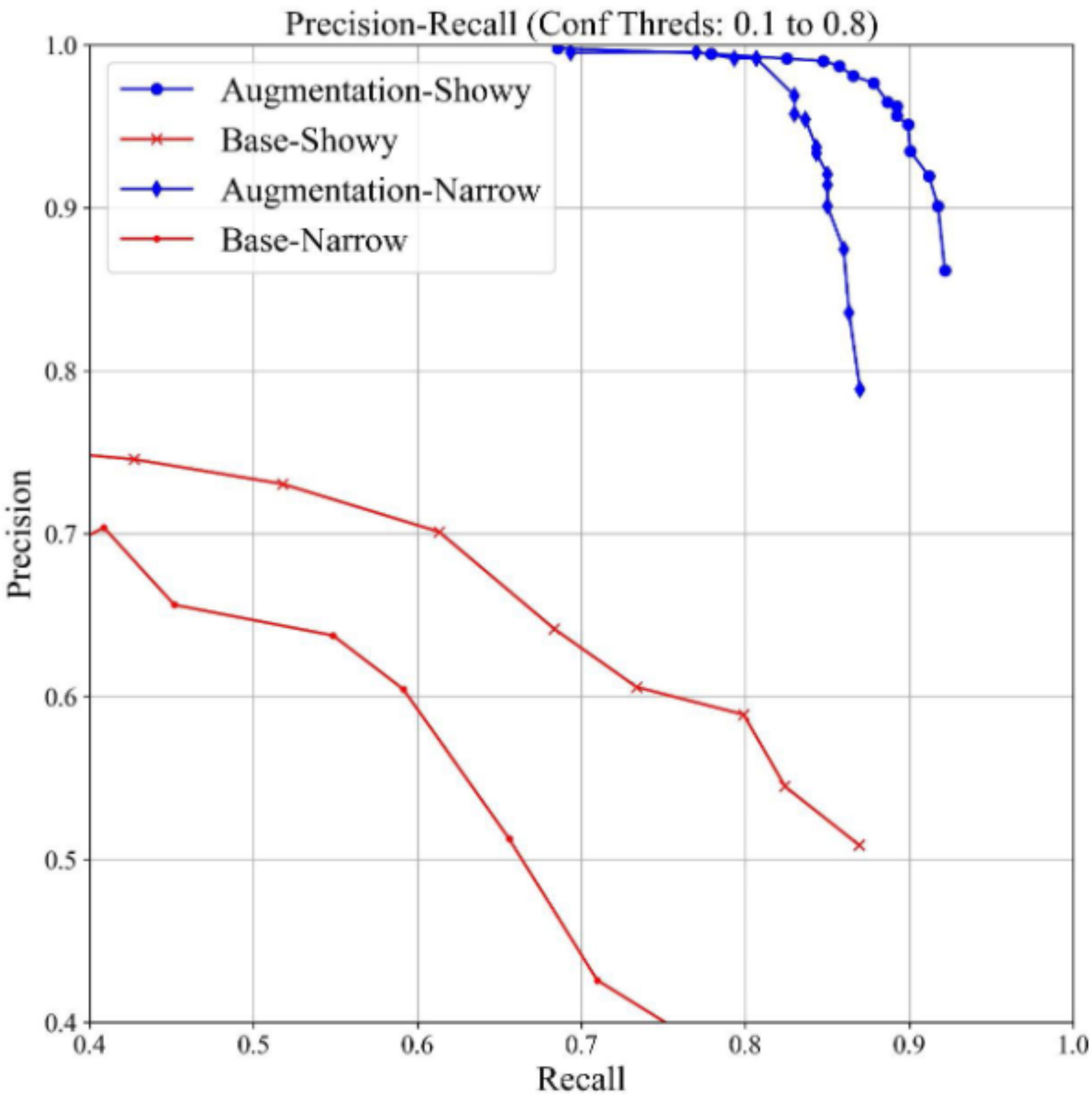


Difference in precision and recall for model using image augmentation (blue lines) and those without image augmentation (red lines).

**Figure 9**

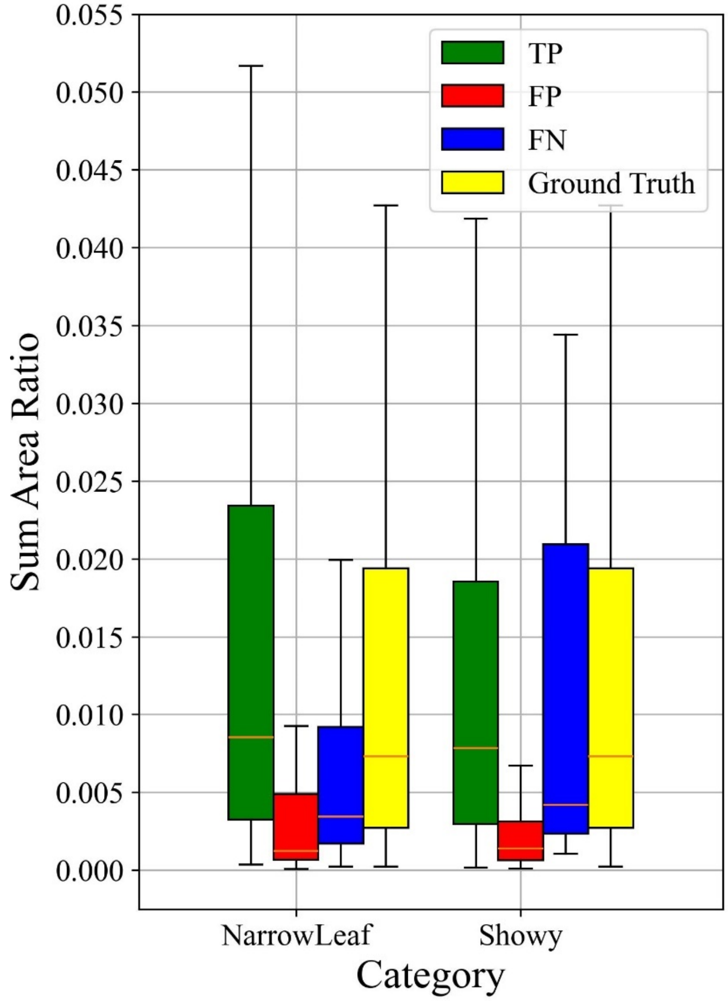


Sum Area Ratio (proportion of the area of each image occupied by milkweed bounding boxes) for narrowleaf and showy detections showing true positive detections, false positives, and false negatives. A proportion of 0.005 corresponds with 0.5% of the image.

**Figure 10**

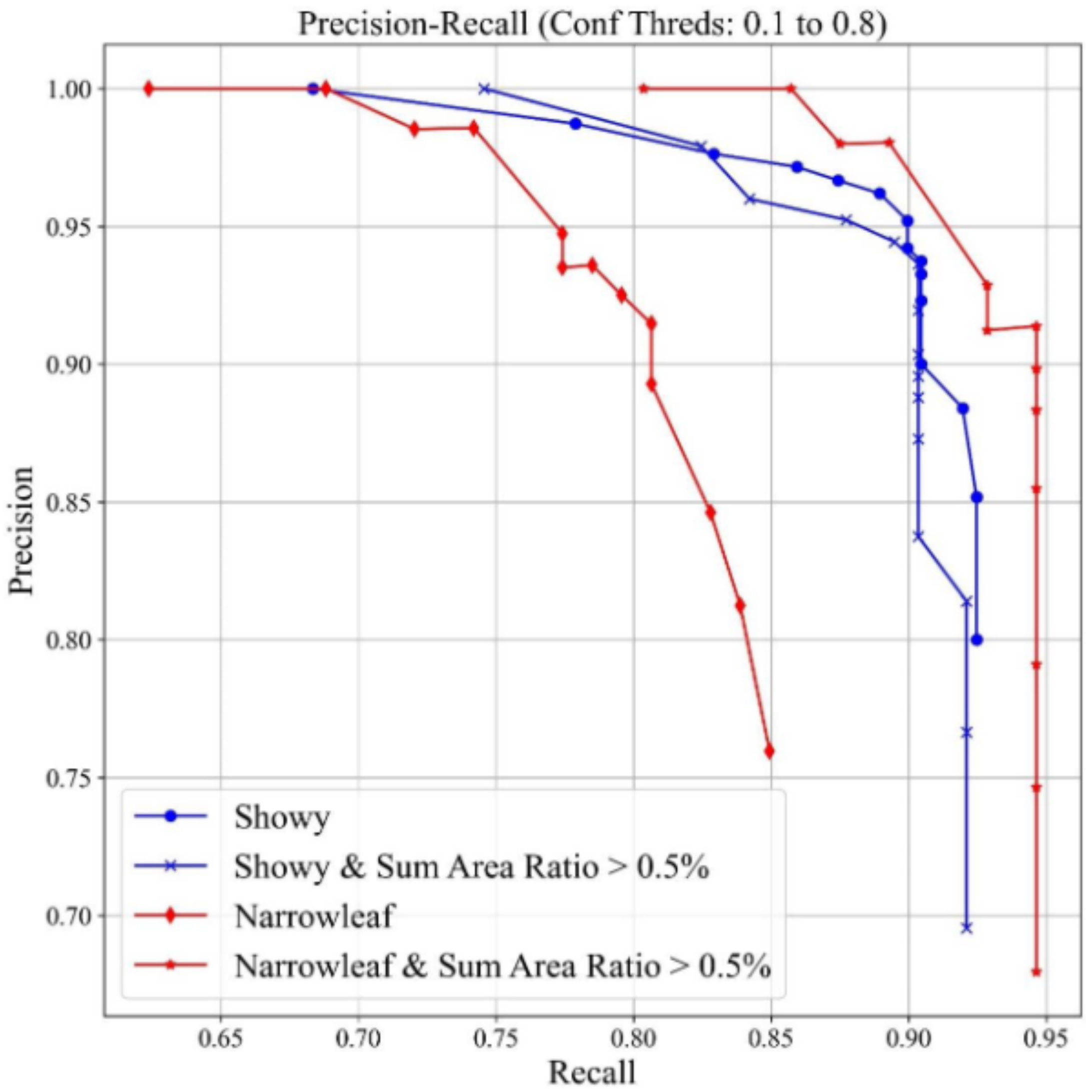


Difference in precision and recall for models that filter images using a threshold of 0.5% of the image as milkweed

**Figure 11**


Examples of correct (A and B) and incorrect (C-F) roadside milkweed classification from the YOLO model for showy milkweed (A, C, and E) and narrowleaf (B, D, and F) milkweed. Incorrect identifications included false positives (C and D) and false negatives (E and F). In example C the model has flagged a sunflower as a showy milkweed. In example D the model has flagged sunflower species as narrowleaf milkweed. In example E the model failed to identify a showy milkweed on the other side of the irrigation ditch. In example F the model failed to identify a narrowleaf milkweed in a pasture. In the right corner of each image a close-up of what the model was identifying, or failing to identify for the false negatives, has been provided.

**Figure 12**

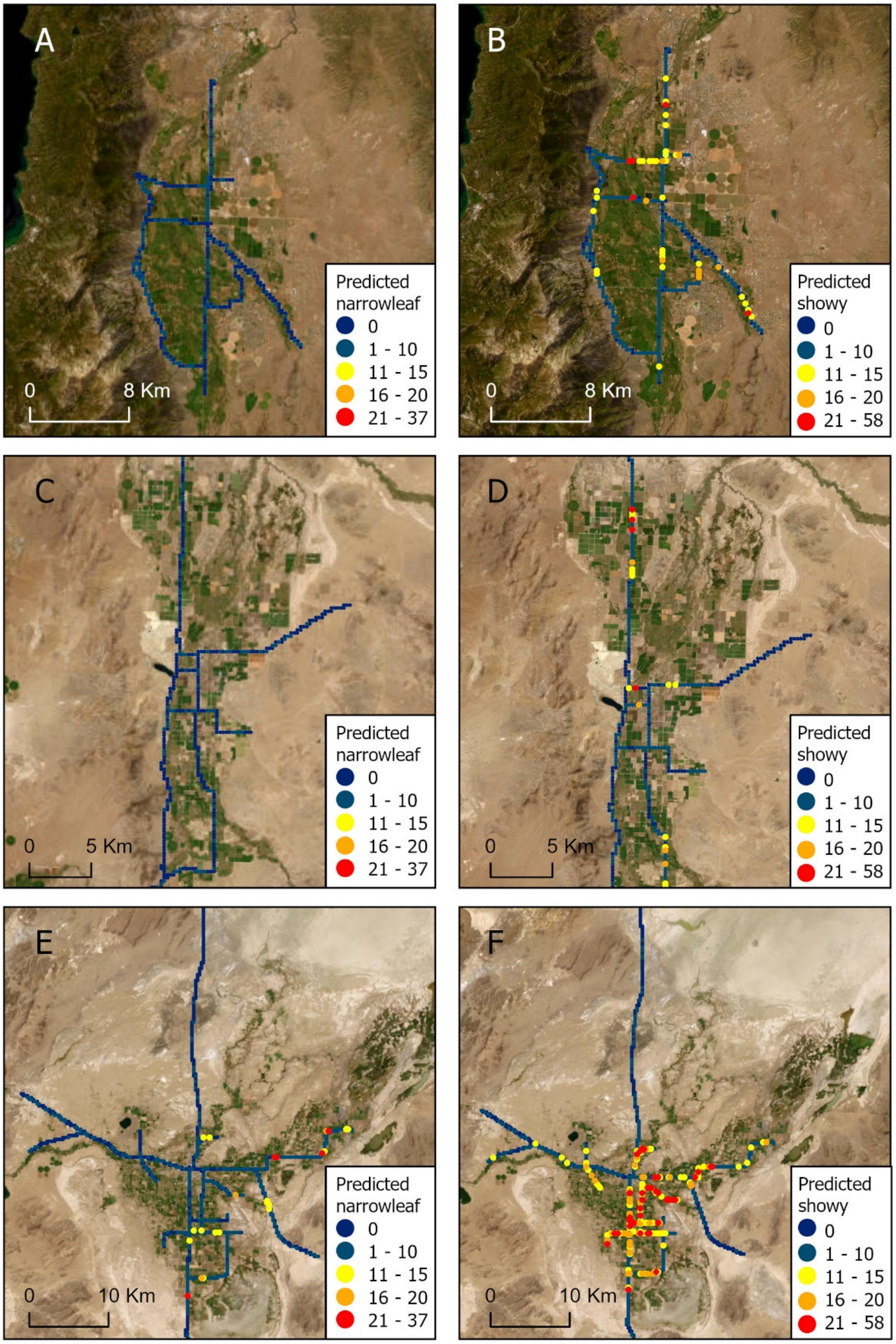


Maps showing the number of predicted milkweed occurrences within a 250x250 meter grid cell for each of the three study area valleys (Carson A and B), Mason (C and D), and Lahontan (E and F). Narrowleaf milkweed is shown in A, C, and E and showy milkweed in B, D, and F.

## REFERENCES


Ali, M. L., & Zhang, Z. (2024). The YOLO framework: A comprehensive review of evolution, applications, and benchmarks in object detection. *Computers*, *13*(12), 336.

Bakacsy, L., Z. Tobak, B. van Leeuwen, P. Szilassi, C. Biró, and J. Szatmári. 2023. Drone-Based Identification and Monitoring of Two Invasive Alien Plant Species in Open Sand Grasslands by Six RGB Vegetation Indices. Drones 7:207.

Bates, D., M. Mächler, B. Bolker, and S. Walker. 2015. Fitting Linear Mixed-Effects Models Using lme4. Journal of Statistical Software 67:1–48.

Behera, T. K., S. Bakshi, and P. K. Sa. 2023. A Lightweight Deep Learning Architecture for Vegetation Segmentation using UAV-captured Aerial Images. Sustainable Computing: Informatics and Systems 37:100841.

Bhatnagar, S., L. Gill, and B. Ghosh. 2020. Drone Image Segmentation Using Machine and Deep Learning for Mapping Raised Bog Vegetation Communities. Remote Sensing 12:2602.

Blaschke, T. 2010. Object based image analysis for remote sensing. ISPRS Journal of Photogrammetry and Remote Sensing 65:2–16.

Bothmann, L., Wimmer, L., Charrakh, O., Weber, T., Edelhoff, H., Peters, W., ... & Menzel, A. (2023). Automated wildlife image classification: An active learning tool for ecological applications. Ecological Informatics, 77, 102231.

Breiman, L. 2001. Random Forests. Machine Learning 45:5–32.

Brooks, M. E., K. Kristensen, J. Koen, A. Magnusson, C. W. Berg, A. Nielsen, H. J. Skaug, M. Maechler, and B. M. Bolker. 2017. (glmmTMB) Balances Speed and Flexibility Among Packages for Zero-inflated Generalized Linear Mixed Modeling. The R Journal 9:378–400.

Burr, A., Schaeg, N., & Hall, D. M. (2018). Assessing residential front yards using Google Street View and geospatial video: A virtual survey approach for urban pollinator conservation. Applied Geography, 92, 12-20.

Cariveau, A. J. B., Haynes, G. A., Perish, P., Tuerk, K., Nootenboom, C., Mitchell, T., ... & Snell-Rood, E. C. (2024). Host plants and landscape predict use of roadside habitat by breeding monarchs. Insect Conservation and Diversity.

Cariveau, A. B., Holt, H. L., Ward, J. P., Lukens, L., Kasten, K., Thieme, J., ... & Oberhauser, K. (2019). The integrated monarch monitoring program: from design to implementation. Frontiers in Ecology and Evolution, 7, 167.

Christin, S., Hervet, É., & Lecomte, N. (2019). Applications for deep learning in ecology. Methods in Ecology and Evolution, 10(10), 1632-1644.

Conciatori, M., N. T. C. Tran, Y. Diez, A. Valletta, A. Segalini, and M. L. Lopez Caceres. 2024. Plant Species Classification and Biodiversity Estimation from UAV Images with Deep Learning. Remote Sensing 16:3654.

Crone, E. E., E. M. Pelton, L. M. Brown, C. C. Thomas, and C. B. Schultz. 2019. Why are monarch butterflies declining in the West? Understanding the importance of multiple correlated drivers. Ecological Applications 29:1–13.

d'Andrimont, R., Yordanov, M., Lemoine, G., Yoong, J., Nikel, K., & Van der Velde, M. (2018). Crowdsourced street-level imagery as a potential source of in-situ data for crop monitoring. Land, 7(4), 127.

Diethelm, A. C., G. M. Mizell, C. Gosse, and E. G. Pringle. In review. Food-plant-associated predation risk and its impact on larval development and adult morphology in the monarch butterfly (Danaus plexippus).

Diethelm, A. C., M. Reichelt, T. E. Dilts, J. P. Farlin, A. Marlar, and E. G. Pringle. 2022. Climatic history, constraints, and the plasticity of phytochemical traits under water stress. Ecosphere 13:e4167.

Dilts, T. E., Steele, M. O., Engler, J. D., Pelton, E. M., Jepsen, S. J., McKnight, S. J., ... & Forister, M. L. (2019). Host plants and climate structure habitat associations of the western monarch butterfly. Frontiers in Ecology and Evolution, 7, 188.

Esri. 2024. ArcGIS Pro. Environmental Systems Research Institute, Redlands, California.

Flockhart, D. T. T., J.-B. Pichancourt, D. R. Norris, and T. G. Martin. 2015. Unravelling the annual cycle in a migratory animal: breeding-season habitat loss drives population declines of monarch butterflies. Journal of Animal Ecology 84:155–165.

Friedman, J., T. Hastie, and R. Tibshirani. 2010. Regularization Paths for Generalized Linear Models via Coordinate Descent. Journal of Statistical Software 33:1–22.

Gautam, D., Z. Mawardi, L. Elliott, D. Loewensteiner, T. Whiteside, and S. Brooks. 2025. Detection of Invasive Species (Siam Weed) Using Drone-Based Imaging and YOLO Deep Learning Model. Remote Sensing 17:120.

Halsch, C. A., Code, A., Hoyle, S. M., Fordyce, J. A., Baert, N., & Forister, M. L. (2020). Pesticide contamination of milkweeds across the agricultural, urban, and open spaces of low-elevation northern California. *Frontiers in Ecology and Evolution*, *8*, 162.

Harris, K. M., Hall, D. M., & Finke, D. L. (2023). Who cares about monarch butterflies? Comparing US State Wildlife Action Plans 2015–2025. Conservation Letters, 16(6), e12976.

Hesselbarth, M. H., Sciaini, M., With, K. A., Wiegand, K., & Nowosad, J. (2019). landscapemetrics: an open-source R tool to calculate landscape metrics. Ecography, 42(10), 1648-1657.

Hosseiny, B., H. Rastiveis, and S. Homayouni. 2020. An Automated Framework for Plant Detection Based on Deep Simulated Learning from Drone Imagery. Remote Sensing 12:3521.

Jocher, G. and Ultralytics. 2025. YOLOv5. Ultralytics.

Kasten, K., Stenoien, C., Caldwell, W., & Oberhauser, K. S. (2016). Can roadside habitat lead monarchs on a route to recovery?. Journal of Insect Conservation, 20, 1047-1057.

Knight, S. M., Norris, D. R., Derbyshire, R., & Flockhart, D. T. (2019). Strategic mowing of roadside milkweeds increases monarch butterfly oviposition. *Global Ecology and Conservation*, *19*, e00678.

Kotowska, D., Pärt, T., & Żmihorski, M. (2021). Evaluating Google Street View for tracking invasive alien plants along roads. Ecological Indicators, 121, 107020.

Lalonde, S., J. L. McCune, S. A. Rivest, and H. M. Kharouba. 2022. Decline in Common Milkweed along Roadsides Around Ottawa, Canada. Ecoscience 29:25–37.

Laumer, D., Lang, N., van Doorn, N., Mac Aodha, O., Perona, P., & Wegner, J. D. (2020). Geocoding of trees from street addresses and street-level images. ISPRS Journal of Photogrammetry and Remote Sensing, 162, 125-136.

Liu, Y., Diao, C., Mei, W., & Zhang, C. (2024). CropSight: Towards a large-scale operational framework for object-based crop type ground truth retrieval using street view and PlanetScope satellite imagery. ISPRS Journal of Photogrammetry and Remote Sensing, 216, 66-89.

Lukas, P., L. Georg, M. Neumann, F. Martin, A. Frey, A. Stoll, and V. Schmidt. 2020. Detection of Colchicum autumnale in drone images, using a machine-learning approach. Precision Agriculture 21:1291–1303.

Lumnitz, S., Devisscher, T., Mayaud, J. R., Radic, V., Coops, N. C., & Griess, V. C. (2021). Mapping trees along urban street networks with deep learning and street-level imagery. ISPRS Journal of Photogrammetry and Remote Sensing, 175, 144-157.

McGarigal, K. (2015). FRAGSTATS help. University of Massachusetts: Amherst, MA, USA, 182.

Murphy, A. W., & Crone, E. E. (2025). Pollinator gardening is constrained by income but not lot size in urban front yards. *Landscape and Urban Planning*, *256*, 105271.

OpenGIS.ch. 2023. QField. OpenGIS.ch.

Ozcan, K., Sharma, A., Bradbury, S. P., Schweitzer, D., Blader, T., & Blodgett, S. (2020). Milkweed (Asclepias syriaca) plant detection using mobile cameras. Ecosphere, 11(1), e02992.
Pardo-Primoy, D., & Fagúndez, J. (2019). Assessment of the distribution and recent spread of the invasive grass Cortaderia selloana in Industrial Sites in Galicia, NW Spain. Flora, 259, 151465.
Pelton, E., McKnight, S., Fallon, C., Code, A., Hopwood, J., Hoyle, S., ... & Black, S. H. (2018). Managing for monarchs in the west: best management practices for conserving the monarch butterfly and its habitat. https://xerces. org/wp-content/uploads/2018/04/18-009_01-Monarch_BMPs_Final_Web. pdf (accessed Sep 2018). Portland (OR): Xerces Society for Invertebrate Conservation, 116.
Pelton, E. M., Schultz, C. B., Jepsen, S. J., Black, S. H., & Crone, E. E. (2019). Western monarch population plummets: status, probable causes, and recommended conservation actions. Frontiers in Ecology and Evolution, 7, 258.
Pillai, R., Sharma, N., Upadhyay, D., Dangi, S., & Gupta, R. (2024, March). Precision in Biometric Authentication: CNN-driven Fingerprint Classification. In 2024 3rd International Conference for Innovation in Technology (INOCON) (pp. 1-5). IEEE.
Pix4D SA. 2023. Pix4D. Pix4D SA.
Pleasants, J. M., and K. S. Oberhauser. 2013. Milkweed loss in agricultural fields because of herbicide use: effect on the monarch butterfly population. Insect Conservation and Diversity 6:135–144.
QGIS Development Team. 2023. QGIS Geographic Information System. Open Source Geospatial Foundation.
R Core Team. 2024. R: A language and environment for statistical computing. R Foundation for Statistical Computing, Vienna, Austria.
Redmon, J. (2016). You only look once: Unified, real-time object detection. In Proceedings of the IEEE conference on computer vision and pattern recognition.
Rillig, M. C., Mansour, I., Hempel, S., Bi, M., König-Ries, B., & Kasirzadeh, A. (2024). How widespread use of generative AI for images and video can affect the environment and the science of ecology. Ecology Letters, 27(3), e14397.
Roboflow. 2024. Roboflow 3.0  https://roboflow.com/ (Last accessed: January 24, 2024)
Rominger, K., and S. E. Meyer. 2019. Application of UAV-Based Methodology for Census of an Endangered Plant Species in a Fragile Habitat. Remote Sensing 11:719.
Salvi, M., Acharya, U. R., Molinari, F., & Meiburger, K. M. (2021). The impact of pre-and post-image processing techniques on deep learning frameworks: A comprehensive review for digital pathology image analysis. Computers in Biology and Medicine, 128, 104129.
Sankey, T., J. Donager, J. McVay, and J. B. Sankey. 2017. UAV lidar and hyperspectral fusion for forest monitoring in the southwestern USA. Remote Sensing of Environment 195:30–43.
Seebach, L., Strobl, P., Vogt, P., Mehl, W., & San-Miguel-Ayanz, J. (2013). Enhancing post-classification change detection through morphological post-processing–a sensitivity analysis. International Journal of Remote Sensing, 34(20), 7145-7162.
Seiferling, I., Naik, N., Ratti, C., & Proulx, R. (2017). Green streets− Quantifying and mapping urban trees with street-level imagery and computer vision. Landscape and Urban Planning, 165, 93-101.
Shorten, C., & Khoshgoftaar, T. M. (2019). A survey on image data augmentation for deep learning. Journal of Big Data, 6(1), 1-48.
Stubbings, P., Peskett, J., Rowe, F., & Arribas-Bel, D. (2019). A hierarchical urban forest index using street-level imagery and deep learning. Remote Sensing, 11(12), 1395.
Torresani, M., D. Kleijn, J. P. R. de Vries, H. Bartholomeus, L. Chieffallo, R. Cazzolla Gatti, V. Moudrý, D. Da Re, E. Tomelleri, and D. Rocchini. 2023. A novel approach for surveying

flowers as a proxy for bee pollinators using drone images. Ecological Indicators 149:110123.
Torresani, M., D. Rocchini, G. Ceola, J. P. R. de Vries, H. Feilhauer, V. Moudrý, H. Bartholomeus, M. Perrone, M. Anderle, H. A. Gamper, L. Chieffallo, E. Guatelli, R. C. Gatti, and D. Kleijn. 2024. Grassland vertical height heterogeneity predicts flower and bee diversity: an UAV photogrammetric approach. Scientific Reports 14:809.
Ulus, A., Yilmaz, H., Akkemik, U., & Yilmaz, O. Y. (2021). Assessing street-Level Distribution of Tree-of-Heaven (Ailanthus altissima) in Istanbul (Turkey). Applied Ecology and Environmental Research, 19(4), 2793-2802.
Valavi, R., J. Elith, J. J. Lahoz-Monfort, and G. Guillera-Arroita. 2021. Modelling species presence-only data with random forests. Ecography 44:1731–1742.
Virtual Surveyor NV. 2023. Virtual Surveyor – Terrain Creator. Virtual Surveyor NV.
Weisberg, P. J., T. E. Dilts, J. A. Greenberg, K. N. Johnson, H. Pai, C. Sladek, C. Kratt, S. W. Tyler, and A. Ready. 2021. Phenology-based classification of invasive annual grasses to the species level. Remote Sensing of Environment 263:112568.
Western Monarch Milkweed Occurrence Database (2018). Data Accessed From the Western Monarch Milkweed Mapper, a Project by the Xerces Society. U.S. Fish and Wildlife Service; Idaho Department of Fish and Game, and Washington Department of Fish and Wildlife. Available online at: https://www.monarchmilkweedmapper.org (accessed January 15, 2017).
Yan, Y., & Ryu, Y. (2021). Exploring Google Street View with deep learning for crop type mapping. ISPRS Journal of Photogrammetry and Remote Sensing, 171, 278-296.

## Nevada Department of Transportation


Tracy Larkin-Thomason, P.E. Director

Lucy Koury, Research Division Chief

(775) 888-7223

lkoury@dot.nv.gov

1263 South Stewart Street

Carson City, Nevada 89712